The Thesis Committee for Michael Thomas O'Connor
Certifies that this is the approved version of the following thesis:

Groundwater dynamics and surface water-groundwater interactions in a prograding delta island, Louisiana, USA

APPROVED BY
SUPERVISING COMMITTEE:

Supervisor:

Kevan B. Moffett

M. Bayani Cardenas

Michael H. Young

Groundwater dynamics and surface water-groundwater interactions in a prograding delta island, Louisiana, USA

by

Michael Thomas O'Connor, B.A.

Thesis

Presented to the Faculty of the Graduate School of

The University of Texas at Austin

in Partial Fulfillment

of the Requirements

for the Degree of

Masters of Science in Geological Sciences

The University of Texas at Austin

May 2014

Acknowledgements

Simply put, the work that comprises this degree would not exist if not for a large and incredible group of people. This work was physically and mentally taxing, and required an enormous amount of support. I was extremely fortunate to have that support in spades, and the people that provided that support deserve acknowledgement beyond what can be provided on this page. First and foremost, to Kevan, my first scientific advisor: I'll bet you had no idea of the headcase you were taking on when you agreed to work with me, but I can't thank you enough for choosing to do so. You have led by example in every possible way, and because of that I think I have quite the excellent model for how I should carry myself in this field (or, frankly, any field). You are going to absolutely knock them dead in Vancouver, and I'm honored and excited that I'll continue to work with you as the transition occurs. Thank you so much. To Bayani and Mike Young, thank you so much for your always helpful comments to both this research and the work I've done in your classes. Your voices have had an enormously positive impact on me as a scientist, and I hope to continue to work with you as I progress. To Brittany, Raquel, Amber, Dylan, Peter, Wayne, and Brandee: congratulations and thank you for surviving the hell on earth that is the Wax Lake Delta. The work simply doesn't happen without your awesome energy helping me out in the field. To my crazy, wonderful family: I'm sorry for moving to Texas, but I am so fortunate for the support you have given and will continue to give me in this new place and new life. You guys define unconditional love, and that's something I can't imagine living without. Lastly, the friends I've made in Austin: Alyse, Brittany, Dylan, Ed, Jenna, Joel, Kenzie, Kim, Kimmy, Peter, Rosemary, and the many others, have made this an experience that I actually want to do again, which, in my understanding of this field, is not always a

guarantee. The time that we get to spend together, talking about science and everything else, directly contributed to the quality and success of this work. I wouldn't be able to make it here in Austin without you. I look forward to many more years of shenanaganry together.

Abstract

Groundwater dynamics and surface water-groundwater interaction in a prograding delta island, Louisiana, USA

Michael Thomas O'Connor, M.S. Geosci

The University of Texas at Austin, 2014

Supervisor: Kevan B. Moffett

Delta islands make up the majority of coastal delta area. However, the groundwater hydrology of young, prograding delta systems and its relationship to surrounding surface water dynamics are poorly understood. Deltas in coastal environments are assumed to function as chemical "buffers", filtering nutrient-rich terrestrial runoff through the island structures and surface water ecosystems as it travels to the sea, but the magnitude of this effect cannot be accurately quantified without understanding the physical relationships between the surface water and groundwater.

This study developed the first conceptual model of the hydrology of prograding delta island groundwater systems. The study was based on field data collected at Pintail Island, a 2 km^2 island within the Wax Lake Delta in Louisiana. Hydraulic properties and processes were quantified at multiple depths at locations spanning the island elevation gradient. Groundwater and surface water levels were monitored. A weather station recorded precipitation, air, and wind conditions.

The groundwater within Pintail Island was both spatially and temporally dynamic throughout the study period of Sept/9/2013 to Feb/4/2014. The aquifer within the distal limbs of the island responded as a connected, saturated unconfined aquifer. The portions of Pintail Island within the older, proximal, higher elevation apex were found to be a two-layer system with fine sediments and organic matter overlying sandy deposits. The aquifer within this section of the island responded differently during times of elevated surface water (storm events) and times of normal surface water (calm periods) and differently from the distal-island unconfined system. The fine, shallow (roughly 0-60cm depth) sediments capping this older, higher portion of the island appeared to inhibit vertical flow between the surface and subsurface, creating semi-confined conditions within the sands in the deeper island subsurface. High water levels led to overpressurization of the apical aquifer, which was maintained between storms due to the low hydraulic gradient and the low permeability of the porous medium. During inundating storm events, groundwater potentials mimicked surrounding surface water levels. This conceptual model of a prograding coastal delta island now provides a foundation for further, hydrologically-realistic study of delta ecology and nutrient exchange.

Table of Contents

List of Tables

List of Figures

	Calm Data Set									Stormy Data Set								
	Shallow Piezometer									*Shallow Piezometer*								
Well	***N1***	***N2***	***N3***	***M1***	***M2***	***L1***	***L2***	***L3***	***DL1***	***N1***	***N2***	***N3***	***M1***	***M2***	***L1***	***L2***	***L3***	***DL1***
Correlation	0.19	0.09	0.23	0.19	0.11	0.52	0.60	0.51	0.53	0.35	0.36	0.35	0.49	0.46	0.66	0.84	0.71	0.77
	Deep Piezometer									*Deep Piezometer*								
Well	***N1***	***N2***	***N3***	***M1***	***M2***	***L1***	***L2***	***L3***	***DL1***	***N1***	***N2***	***N3***	***M1***	***M2***	***L1***	***L2***	***L3***	***DL1***
Correlation	0.25	0.06	0.20	0.07	0.12	0.61	0.68	0.98	0.61	0.32	0.26	0.43	0.32	0.44	0.80	0.85	0.98	0.76

1. Introduction

Deltaic environments are of significant anthropogenic interest. Fertile, water-rich delta plains are home to over 500 million people worldwide and provide food for millions more (Syvitski and Saito, 2007). Society and agriculture both rely heavily on freshwater sources and often groundwater supplies much of that demand (Siebert et al., 2010). However, these environments, often characterized by large deposits of unconsolidated sediment, can be subject to significant subsidence from groundwater pumping (Stanley, 1990; Alam, 1996). Coastal deltas are additionally affected by rising sea levels due both to anthropogenic climate change (Day et al., 2000; Reed, 2002), compaction of sediment, and extraction of underground fluids (Wada et al., 2012). These factors could potentially alter the physical and chemical properties of delta groundwater and highlight why a complete understanding of delta groundwater systems and surface water/groundwater dynamics is important.

The geomorphology of a river delta dictates the eventual hydrogeologic properties of the system (Li et al., 2009), yet the groundwater dynamics of young delta islands and their co-evolving interactions with surface water dynamics and sediment deposition remain an open question. River deltas develop in distinct island-channel patterns, and the specific mechanisms for how these patterns develop are the subject of much active research (Slingerland and Smith, 2004; Parker and Sequeiros, 2006; Kim et al., 2009; Shaw et al., 2013). Delta systems tend to be aerially extensive and low relief. Therefore, small fluctuations in surface water level can significantly alter the amount of exposed land within the system (Branhoff, 2012; Hiatt et al., 2014). Additionally, river deltas develop well-stratified sedimentological regimes in the subsurface, as variations in surface water velocities during depositional events within the delta lead to the well-sorted

deposition of different-sized particles (Roberts et al., 1997). This stratification often results in a general sediment regime where grain sizes increases with depth (Nichols, 2013).

These morphological properties of prograding coastal deltas have hydrologic and hydrogeologic implications. The low relief of the delta could allow for frequently varying surface water/groundwater exchange, which influences groundwater flow paths (Harvey et al., 1987; Bardini et al., 2012). Changing groundwater conditions will also influence biogeochemistry, as the amounts of available oxygen, dissolved organic carbon, and nutrients, for example, in any particular region of the subsurface may change with inundation (Postma et al., 1991; Bardini et al., 2012). Additionally, the variable sediment structure present in deltaic environments could lead to differential groundwater flow velocities and thus affect surface water/groundwater interactions. For example, investigations into a South Carolina salt marsh showed that the presence of a lower permeability sediment layer at the surface of the marsh decreased the vertical connectivity between the surface hydrology and shallow subsurface hydrology, and that the dominant hydrologic forcings in this system were lateral (Wilson et al., 2011).

Considering that delta islands compose the majority of surface area within a delta, understanding the groundwater dynamics within these islands and their interactions with the surrounding channels is a critical component of a comprehensive understanding of deltas on the whole. However, this remains poorly understood for the coastal delta setting. Although there is a lack of literature examining groundwater systems in prograding coastal delta islands, a number of near-analogues have been studied. Inland deltas, such as the Okavango Delta in Botswana, and ancient coastal deltas such as the Nile Delta in Egypt and the Ganges/Brahmaputra Delta in India and Bangladesh have

been investigated for groundwater contamination and subsidence reasons related to modern anthropogenic presence (Stanley, 1990; Alam, 1996; McCarthy, 2006). These cases differ from prograding delta islands in that prograding delta islands are rarely inhabited and so do not experience anthropogenic pumping. Also, ancient and inland deltas are not as dominated by modern coastal surface water forcings as coastal, rapidly prograding deltas. Various investigations have shown tides and onshore/offshore wind patterns to be a significant driver of surface water fluctuations in coastal delta systems (Habib and Meselhe, 2006; Snedden, 2006; Geleynse et al., 2014; Hiatt et al., 2014). Since island groundwater is directly connected to nearby surface water, it is reasonable to believe these coastal forcings will play a significant role in describing the groundwater system in coastal delta islands.

Fluvial island bars and barrier islands are also near-analogues for delta islands. Like coastal delta islands, they are strongly influenced by surface water conditions and are highly sensitive to small surface water changes. They have been investigated as potential locations for natural nutrient processing due to changing redox conditions (Anschutz et al., 2009). Fluctuations in river stage (surface water level) lead to different zones of inundation within a fluvial or barrier island (Anschutz et al., 2009; Cardenas, 2010; Cardenas and Jiang, 2011; Bardini et al., 2012). In barrier islands, the consistent ocean wave action provides the potential for rapid surface water/groundwater exchange at the island margins and causing lateral groundwater pulses that dissipate as the pulse moves inland (Li and Barry, 2000; Horn, 2002). Coastal delta islands have the potential to exhibit similar lateral pressure responses. However, fluvial islands and barrier islands differ from coastal delta islands in their sedimentology, tending to be of more poorly sorted and coarse grain sizes (Nichols, 2013). Additionally, barrier islands are

surrounded by saline surface water, which influences the groundwater geochemistry and island ecology (Reide Corbett et al., 2000; William P. Anderson, 2002; Röper et al., 2012). This also departs from rapidly prograding coastal deltas, which generally are freshwater-dominated systems due to their large, sustained continental discharge volumes (e.g., Shaw et al., 2013).

The sedimentology of salt marshes and coastal delta islands can be similar. Like many delta islands, salt marsh sedimentology can generally be described as fining upwards, with coarser sediments overlain by fine organic matter and mud (e.g., Hughes et al., 1998; Wilson et al., 2011). As described above, geomorphology can strongly control the groundwater dynamics in a sedimentary system (Li et al., 2009). Investigations into salt marsh hydrology have shown that the hydraulic conductivity of the sediment directly influences groundwater flowpaths and surface water/groundwater interactions (Hughes et al., 1998; Moffett et al., 2012), and that low conductivity sediments in a region of significant plant transpiration can lead to aeration 'pockets' within the otherwise saturated salt marsh (Ursino et al., 2004; Zhang et al., 2013). However, the salinity of salt marshes greatly affects both the physics and chemistry of the groundwater within the marsh; these effects will not be seen in a freshwater-dominated system such as a coastal delta.

The ecosystem services provided by a coastal delta also distinguish it from its near-analogues. Coastal deltas are often the recipients of large volumes of continental runoff, much of which carries high concentrations of nitrate and phosphate from agricultural runoff (Goolsby et al., 2000). As the terminus of this runoff, the coastal delta plain receives these high-nutrient inputs and provides a final opportunity for those nutrients to be consumed through microbial metabolism in benthic, hyporheic, and bank

sediments, as well as slow-flowing wetland water columns, prior to discharge to the sea (Spalding and Parrott, 1994; Musslewhite et al., 2003; Rivera-Monroy et al., 2010). Many land management policies crafted today consider the potential for these processes to occur on a large scale: for example, the Louisiana Coastal Master Plan of 2012 cites the development of new coastal wetland area as a potential remedy to the growing anoxic zone in the Gulf of Mexico ("Louisiana's 2012 Coastal Master Plan."; Rabalais et al., 1996). The nutrient-buffering capacity of coastal wetland and delta systems continues to be an active area of research (Venterink et al., 2003; Rivera-Monroy et al., 2010; Henry, 2012), yet there is, so far, little research attempting to connect the nutrient buffering capacity of these systems with their groundwater hydrology.

An accurate understanding of the groundwater dynamics within a delta island is necessary both to describe a currently unknown process and to develop realistic biogeochemical reaction estimates within such systems. This study identified the key controls on the groundwater dynamics of a prograding island in a river-dominated coastal delta undisturbed by anthropogenic interference. Time-series data of groundwater and surface water potentials across space and time within and around an island were analyzed and compared to environmental forcing factors such as onshore/offshore winds, tides, river discharge, and rain events. Existing sedimentological data were combined with new observations to characterize the hydrogeologic structure and flow systems within the island and to identify their connections to the surface water dynamics.

2. Study Site and Methods

2.1 Study Site

The Wax Lake Delta (29.5226° N, 91.4367° W) is a roughly 100 km2 rapidly prograding delta 130 km southeast of New Orleans, LA. It is characterized by large, chevron-shaped islands and narrow channels. It is fed by the Wax Lake Outlet, a man-made channel excavated in 1941 by the US Army Corps of Engineers (Roberts et al., 1997). The Wax Lake Outlet is fed by the Atchafalaya River and receives roughly 10% of the total water flow of the Mississippi River system (Parker and Sequeiros, 2006). Although the delta protrudes into Atchafalaya Bay, salinity measurements are very low for many kilometers beyond the delta shoreline, making it a freshwater-dominated system (Shaw et al., 2013). Atchafalaya Bay is a shallow platform, with an average depth of roughly 2 m (Neill and Allison, 2005). The Wax Lake Delta developed subaqueously from 1941 until 1973; in 1973, a large flood delivered enough sediment to the system that it became subaerial (Wellner et al., 2005).

This study focused on Pintail Island, one of the older islands in the Delta (Figure 1). Pintail Island is a roughly 2 km^2 island, 0.7 km wide at its widest point and 3.2 km long along its major axis. The relief of the island, from the highest to lowest points in a 2009 Lidar survey (NCALM, 2009), is roughly 50 cm. The island vegetation zonation follows its elevation profile, with the highest island elevations dominated by *Salix nigra* (black willow), *Colocasia esculenta* (elephant ear) at slightly lower elevations, and *Nelumbo lutea* (lotus) and various reed species in the often-flooded, lower elevation, inner island (Viparelli et al., 2011) (Figure 2). The oldest parts of Pintail Island are nearest to its apex (north), and the youngest parts are farthest toward the bay (south). The

island surrounds a shallow lagoon that, at its northernmost points, is heavily vegetated and becomes exposed low-marsh at times of low water.

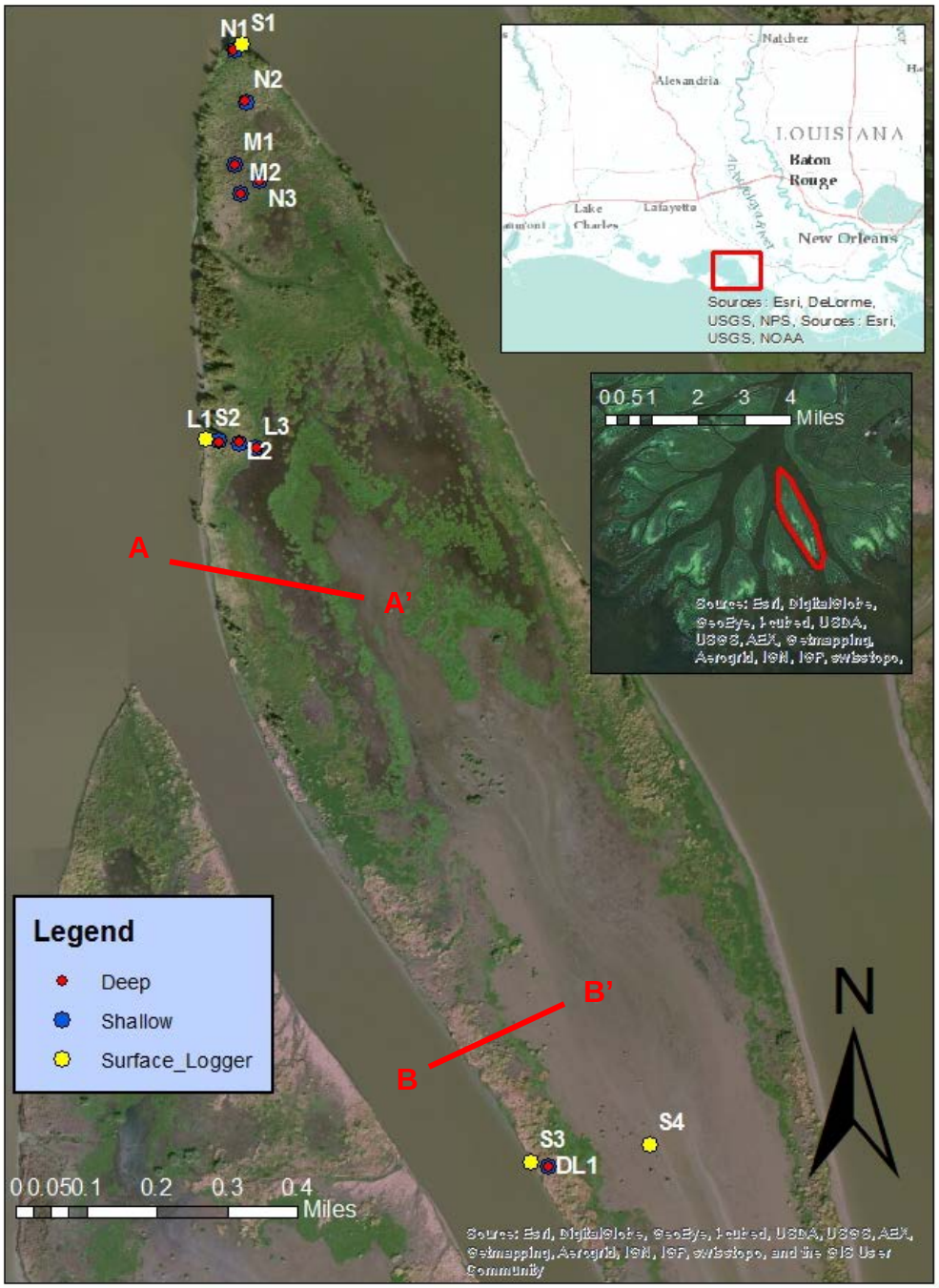

Figure 1: Map of Pintail Island and well/sample locations and location of Pintail Island within both the Wax Lake Delta and Louisiana. Cross-sections denoted correspond to generalized cross-sections in Figure 2. Background imagery from ESRI.

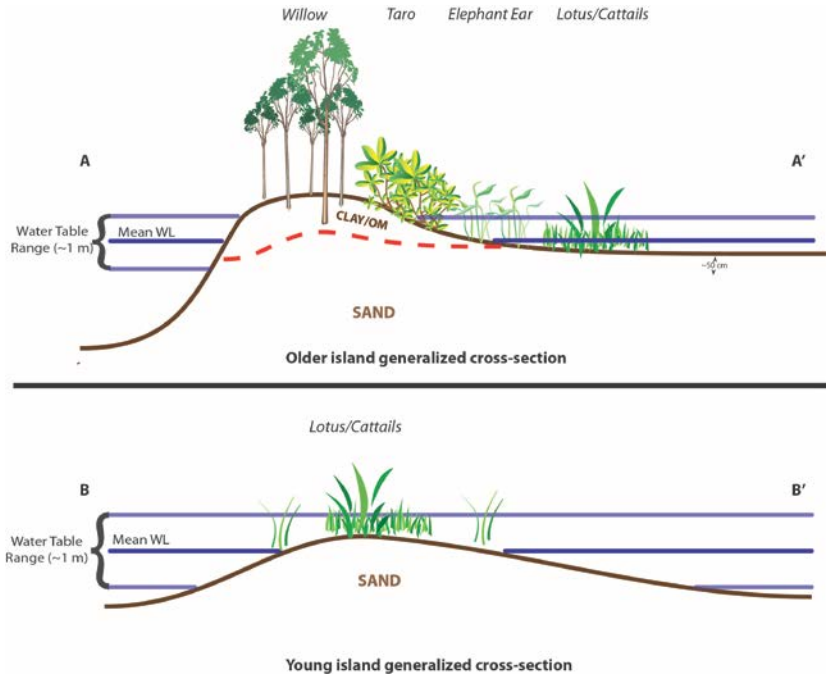

Figure 2: Generalized up- and down-island cross sections with schematic sediment properties and vegetation as denoted from Figure 1

Prior studies of the surface water dynamics of Wax Lake Delta documented a 20-30 cm microtide (Wellner et al., 2005) and an often more substantial surface water influence by onshore and offshore winds (Geleynse et al., 2014). These tide and wind influences were also confirmed for the inner-island lagoon of Pintail Island, which detains a significant amount of surface water flow from the channels (Hiatt, 2014).

For this study, information on surface water were obtained from publically available sources: the NOAA regional tide prediction dataset for Point Cheveruil, LA (10.6 km west of the Pintail Island apex) (NOAA, 2014) and discharge data for the Atchafalaya River (of which 30 percent of its flow is partitioned to the Wax Lake Outlet in this study (Neill and Allison, 2005)) was garnished from the USGS Gage Station at Simmesport, LA (ID # 07381490) (USGS, 2014).

2.2 FIELD METHODS

To roughly identify the stratigraphic structure of the shallow island sediments, a coarse survey was conducted on Pintail Island using an Eijenkamp Cone Penetrologger. This device measures instantaneous resistance to penetration in a 1D profile of 80 cm depth, which allows for rapid estimation of subsurface grain size at many locations. The island was surveyed at 15 points near hydraulic monitoring locations (described below). At each point, five replicate penetrologger trials were performed. The penetrologger was pushed at a constant speed of 2 cm/s and the cone diameter was 5 cm. Undisturbed sediment samples were collected at 20 cm and 70 cm depth a location near well pairs L1 and analyzed using a Decagon Hyprop and associated softare (Decagon Devices, Inc., Pullman, WA), to determine a soil water retention curve and hydraulic properties of the soils.

To measure environmental factors at the island, a micro-meteorological station (Onset HOBO, Bourne, MA) was installed at the apex of the island near well pair N2. It was placed away from trees at a horizontal distance roughly three times the height of the tallest nearby willows. The weather station recorded at 3 m altitude, precipitation, wind speed and wind direction, shortwave and photosynthetically active solar radiation fluxes, humidity, air temperature, and atmospheric pressure every 5 minutes.

The groundwater table and surrounding surface water levels were monitored over time by a network of piezometers and data loggers. Piezometer pairs were placed into four general transects (Figure 1), and each pair included a shallow and a deep piezometer. For convenience, these short-screened and vertically nested piezometers will be referred to as ‘wells’ for the remainder of this study. The method of installation was as follows. First, a penetrometer survey was conducted to determine a local sediment profile. The

sediment survey determined the ‘shallow’ and ‘deep’ locations of interest based on preliminary observations: the shallow well was placed at a depth with a high resistance to penetration, generally 40-60 cm deep, and the ‘deep’ well was placed at the depth with a low resistance to penetration, generally about 80-100 cm deep. For each well, a hole was augered to this depth of interest and a well, comprised of a 5 cm-diameter PVC pipe attached to an 18 cm-long well screen, was installed with coarse sand around the screen and the annulus backfilled with native silty-clay. Casings were extended above ground level to prevent flooding of the wells. A pressure transducer (In Situ Level Troll 300, In Situ, Inc., Ft. Collins, CO) was deployed at the bottom of each well. For surface water monitoring stations, an identical pressure transducer was attached to a fencepost driven into the river bottom such that the bottom of the logger was just touching the sediment surface. To compensate for the unvented nature of these data loggers, a barometric pressure logger (BaroTroll, In Situ, Inc., Ft. Collins, CO) was installed at the island apex attached about 2 m above the ground on a large tree. Barometric pressure fluctuations were removed from the surface and groundwater logger data via the automated associated software (Win-Situ v.5, In Situ, Inc., Ft. Collins, CO).The absolute elevation of each logger was determined through a combination of precise kinematic GPS measurements and total station surveying. Three locations on the island were established as base station locations, each with a NetRS High-Precision GPS (Trimble, Sunnyvale, CA). The GPS recorded data points at 5-second intervals for a period of six hours at each of the three locations, which allowed for 2 cm vertical resolution at all points after postprocessing. Postprocessing occurred through the Online Positioning User Service as provided by the National Geodetic Survey (NGS, 2014). Following that, a R3 Total Station (Trimble, Sunnyvale, CA) was installed on the same tripod, and relative locations of groundwater

and surface water locations within sight were surveyed from those base station points. Measurements were taken both to the well measuring point and the ground surface of each well and the difference verified as the exposed casing length.

2.3 DATA PROCESSING

Water levels and environmental variables were compared using correlation and frequency analyses. Linear regressions were performed for two purposes: first, to determine the correlation between a groundwater head signal and the surface water signal nearest to it, and second,to determine the correlation between surface water change and the environmental factors that might cause such change. They were performed between the surface water signal and each groundwater signal and between the surface water or groundwater signals and the environmental variables preciptation and wind speed. The rate at which groundwater head values rose was calculated for each storm event by calculating the linear slope between the local minimum and local maximum groundwater head values. Fast fourier transforms (a.k.a FFT, Oppenheim and Schafer, 2009) were performed using the 'fft' function in MATLAB (Mathworks, Natick, MA) to convert all time series data (groundwater levels, surface water levels, precipitation, and wind speed) to frequency data (as by Hiatt et al. (2014)). FFT were employed in order to identify where dominant periods fell within a large time series dataset. This was done by normalizing the amplitude values within each dataset to determine which time frequencies yielded the most significant periodicity. The normalized FFTs of each dataset were then compared to identify similarities in periodicity within signals, which helped determine how significantly tidal fluctuations, wind speed, precipitation and river discharge contributed to the overall observed surface water signal, and how that surface

water signal contributed to the observed groundwater signals. Frequencies were then converted to periods so that dominant periods of dynamic response within each dataset could be identified.

Preliminary inspection of the collected datasets suggested a strong difference in system response between storm and non-storm events. To analyze this potential difference, the time series were separated based on a wind and rain threshold, where a day was considered 'storm-dominated' if it experienced sustained winds above 5 m/s or rain events exceeding 10 mm/hr. These thresholds were chosen based on the observation that these events caused a significant disruption in the surface water patterns recorded. The above analyses were then performed for three different presentations of data: the entire study period, which extended from September 9, 2013 to February 4, 2014, concatenated storm-dominated days, and concatenated non-storm-dominated days. Using this threshold, the storm data subset covered 28 days, with average wind speed of 1.50 +/- 1.38 m/s and average measured precipitation rate of 5.17 mm/day. The calm data subset covered 85 days, with average wind speed of 1.12 +/- 1.21 m/s and average precipitation rate of 1.41 mm/day.

3. Results

3.1 Surface Water Dynamics

Surface water levels at all loggers showed significant periodicity during both the calm and stormy datasets; however, storm events disturbed that periodicity and raised the local water level overall (Figure 3). Among the loggers located in the main channel adjacent to Pintail Island (S1, S2, and S3), the periodicity coincided in time and the signals showed no noticeable lag. For these reasons, this paper will refer to these signals collectively as the "channel signal" and represent it by the records from S3 in the remainder of the analysis. The water level signal at S4, installed in the island's central lagoon, lagged one hour behind the channel signal.

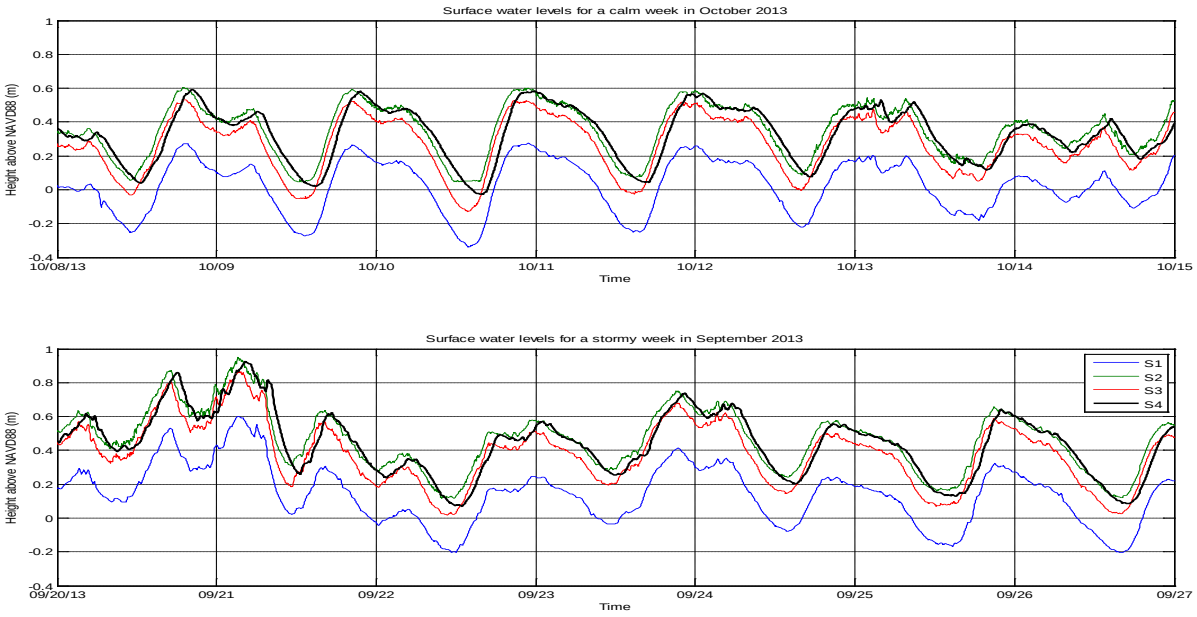

Figure 3: Surface water measurements recorded at all four logger locations for: (top) the calm week of 10/8 to 10/15/2013 and (bottom) for the stormy week of 9/20 to 9/27/2013

Linear regression analyses (Table 1A in Appendix) produced significant correlations ($p < 0.001$) between surface water levels and the NOAA tidal prediction and between surface water levels and wind speed magnitude. No significant correlation was observed between Wax Lake Outlet discharge (which continually increased over the study period) and surface water levels, nor was there a correlation between surface water levels and precipitation.

Fourier analysis of the entire time series (left column, Figure 4) showed the channel signal to be dominated by periods occurring at 12.5, 24, and 25.8-hour intervals. The y-axes in these plots represents the amplitude of a frequency occurring a corresponding period—within these plots, all amplitudes are normalized to the mean amplitude of the dataset. To determine potential sources of these periodicities, the same analysis was performed for the known measurable environmental forcings on surface water: NOAA tide prediction, discharge from the Atchafalaya River, wind speed, and rainfall. That analysis yielded dominant periods of 12.5, 24, and 25.8 hours within the tide prediction, a dominant period of 24 hours within the wind speed signal, and no dominant periods in either discharge or precipitation. These same periodicities dominated the calm-days subset of data (middle column, Figure 4).

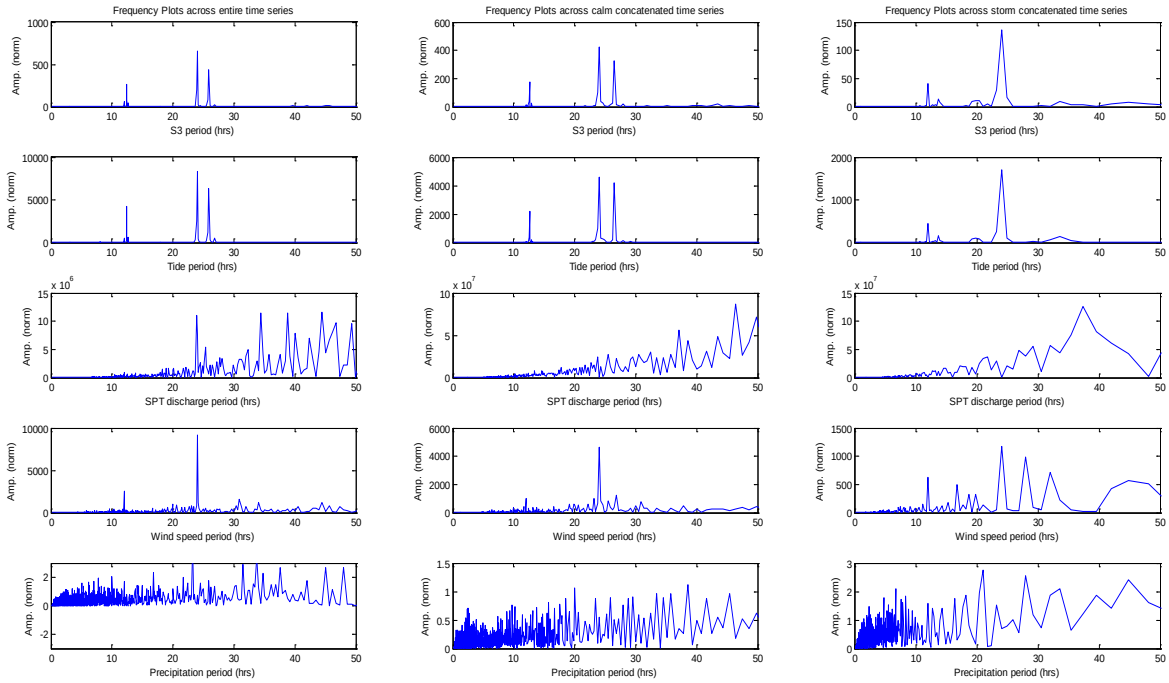

Figure 4: Fourier frequency analysis results, expressed as recurrence period in hours, for surface water and environmental data performed for the entire time series (left column), for concatenated calm days (center column), and for concatenated stormy days (right column). Variables analyzed were: S3, the representative main channel surface water signal (1st row), NOAA predicted tide signal (2nd row), Atchafalaya River discharge (3rd row), and wind speed and precipitation measured on Pintail Island (4th and 5th rows). Y-axes are normalized amplitude (raw amplitude divided by number of records in each dataset.)

The Fourier analysis on the stormy-days subset of data showed that the system behaved differently when perturbed by a storm event. The 12.5 and 25.8-hour signals within both the channel data and the tidal prediction were greatly diminished in magnitude compared to during calm days. Conversely, the highly prominent diurnal (24 hour) signal observed during calm days becomes more pronounced within surface water and tides. In the wind signal, many dominant periods appeared, making the results less conclusive than in calm times; this occurs to a greater extent within the precipitation data,

as many periods are observed within the stormy days subset of data, but none are observed in the calm days subset of data. Outlet discharge did not exhibit any notable periodicity in either subset analysis.

3.2 HYDROGEOLOGY AND GROUNDWATER DYNAMICS

Pintail Island was found to consist of two dominant sediment regimes roughly classified as the 'northern' region and the 'southern' region (Figure 5). The southern portion is relatively homogeneous and coarser-grained, while the northern portion follows a pattern of grain sizes that get finer nearer to the surface (Smith, 2014). Hyprop analysis of sediment samples showed that shallow (0-20 cm) sediments from the northern region were roughly an order of magnitude less conductive than shallow (0-20 cm) sediments from the southern region (1 cm/d versus 0.2 cm/day, respectively, Figure 3A in Appendix). To create the map of Figure 5, it was assumed that the observations of a two-layer system made in the northern portion of the island could be extrapolated to all island elevations above 0.45 m above NAVD88 (NCALM, 2009), which was roughly the lowest elevation point observed above the cut bank. It was then assumed that all observations made in the southern portion of the island, by virtue of falling below this cut bank, could be extrapolated to all island elevations below 0.45 m above NAVD88. Using this threshold and the 2009 Lidar dataset, a generalized delineation between the two zones could be created.

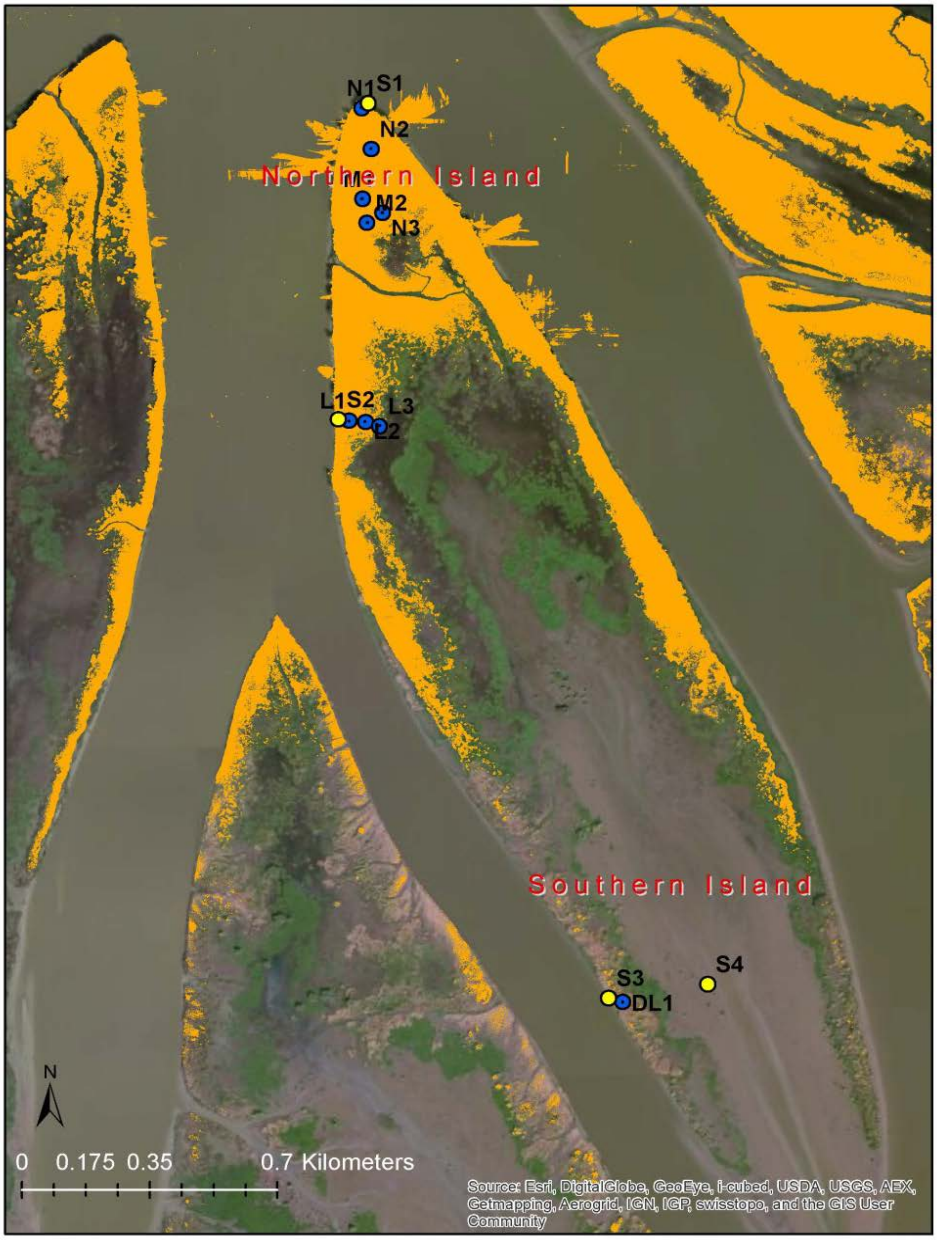

Figure 5: Conceptual map of the shallow (~1 m depth) sedimentology of Pintail Island as determined from the Penetrologger analysis and field observation. A higher-elevation, 'northern island' zone (in orange) generally consists of sands overlain by finer sediments. The lower-elevation, 'southern island' zone is sand bar-like. The southern zone and the central lagoon/mudflat are unshaded. Well pairs are located at blue dots, and surface loggers are located at yellow dots, as in Figure 1, for reference. Background imagery from ESRI

3.2.1 GROUNDWATER HEAD TIME SERIES AND RELATIONSHIP TO SURFACE WATER DYNAMICS

The five-month observation period showed substantial fluctuations in both space and time among well locations in the horizontal and vertical directions, but also highlighted overarching patterns. All data displayed below are derived from the deep well within each well pair for simplicity. This is because for all well pairs excluding pair L2 (which is assumed to have a clogged well), the shallow and deep wells yielded nearly identical signals. This was verified by linearly correlating each shallow well signal to its corresponding deep well signal (Table 1). The entire datasets for both shallow and deep wells are available in the Appendix.

Cluster	***N1***	***N2***	***N3***	***M1***	***M2***	***L1***	***L2***	***L3***	***DL1***
Correlation	0.89	0.86	0.75	0.93	0.99	0.97	0.65	0.98	0.94

Table 1: Correlation coefficients between the shallow and deep wells at each paired well location. Significance is $p < 0.001$ for all calculations. The unusually low correlation at L2 is likely explained by well screen clogging.

Groundwater levels were most responsive to surface water levels at well sites near island edges: N1, L1, L2, L3, and DL1. Within this group, however, there were 'degrees of responsiveness' to the surface water signal. For example, sites N1 and L1 showed a diurnal response to surface water forcing but it was heavily damped and strongly lagged (between 8 and 11 hrs), thus their correlation with surface water was relatively low. Sites L3 and DL1 showed a less lagged and less damped signal, thus their correlation with surface water in both calm and stormy data subsets was higher (Table 2). The extremely high correlations at well L3 deep, in fact, indicate that it behaved as if a stilling well recording the lagoon water level. Inland sites, such as N2, N3, M1, and M2, failed to exhibit fluctuations on the diurnal timescale like the surface water, so correlations were

low. In these inland places, groundwater either remained in apparent hydrostatic equilibrium or was steadily lost to drainage/evapotranspiration after each storm event (see Figure 6). Fourier analysis supported the correlation results, showing prominent periods that matched in surface water and groundwater at 24 and 25.8 hour intervals for wells N1, L1, L2, L3, and DL1 (Figure 7). Such dominant frequencies were absent in the data from inland loggers N2, N3, M1, and M2. Periods of 12 hours were observed at small amplitudes in wells L3 and DL1.

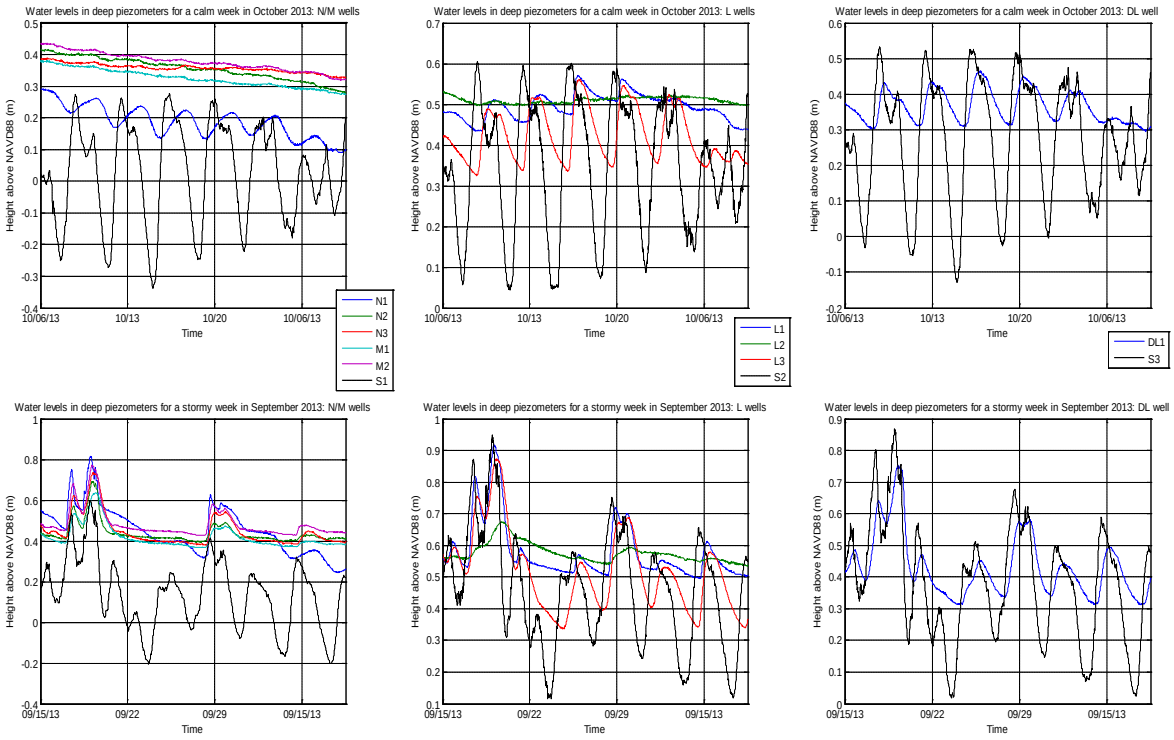

Figure 6: Water level data as recorded from each deep well within each well cluster, (top) for a calm week between 10/8 and 10/15/13, and (bottom) a stormy week between 9/20 and 9/27/13. Columns organize record by transect (see Figure 1).

	Calm Data Set									Stormy Data Set								
	Shallow Piezometer									*Shallow Piezometer*								
Well	***N1***	***N2***	***N3***	***M1***	***M2***	***L1***	***L2***	***L3***	***DL1***	***N1***	***N2***	***N3***	***M1***	***M2***	***L1***	***L2***	***L3***	***DL1***
Correlation	0.19	0.09	0.23	0.19	0.11	0.52	0.60	0.51	0.53	0.35	0.36	0.35	0.49	0.46	0.66	0.84	0.71	0.77
	Deep Piezometer									*Deep Piezometer*								
Well	***N1***	***N2***	***N3***	***M1***	***M2***	***L1***	***L2***	***L3***	***DL1***	***N1***	***N2***	***N3***	***M1***	***M2***	***L1***	***L2***	***L3***	***DL1***
Correlation	0.25	0.06	0.20	0.07	0.12	0.61	0.68	0.98	0.61	0.32	0.26	0.43	0.32	0.44	0.80	0.85	0.98	0.76

Table 2: Correlation coefficients between groundwater signals and the nearest surface water signal, separated for the storm data set and calm data set. Significance is $p < 0.001$ for all calculations.

Groundwater levels were most responsive to surface water levels at well sites near island edges: N1, L1, L2, L3, and DL1. Within this group, however, there were 'degrees of responsiveness' to the surface water signal. For example, sites N1 and L1 showed a diurnal response to surface water forcing but it was heavily damped and strongly lagged (between 8 and 11 hrs), thus their correlation with surface water was relatively low. Sites L3 and DL1 showed a less lagged and less damped signal, thus their correlation with surface water in both calm and stormy data subsets was higher (Table 2). The extremely high correlations at well L3 deep, in fact, indicate that it behaved as if a stilling well recording the lagoon water level. Inland sites, such as N2, N3, M1, and M2, failed to exhibit fluctuations on the diurnal timescale like the surface water, so correlations were low. In these inland places, groundwater either remained in apparent hydrostatic equilibrium or was steadily lost to drainage/evapotranspiration after each storm event (see Figure 6). Fourier analysis supported the correlation results, showing prominent periods that matched in surface water and groundwater at 24 and 25.8 hour intervals for wells N1, L1, L2, L3, and DL1 (Figure 7). Such dominant frequencies were absent in the data from inland loggers N2, N3, M1, and M2. Periods of 12 hours were observed at small amplitudes in wells L3 and DL1.

As in the surface water analysis, the most noticeable temporal observation across all wells was the apparently distinct hydrologic behaviors between storm events and non-

stormy days. All correlations improved during storm events (Table 2). During stormy days, groundwater fluctuations across the island tended to strongly mimic the diurnal behavior of the surrounding surface water, independent of spatial location (Figure 6). Within these relatively brief (1-2 day) periods, the groundwater levels peaked at maximum total head values similar to the nearby surface water stage peaks, but the groundwater peaks lagged by a time interval that increased with well distance from shore. This behavior was also reflected in the correlations between groundwater and surface water signals, which were greater for the stormy data set than for the calm data set (Table 2). Fourier frequency analysis showed that there was a significant 24-hour period across nearly all wells during storm events (Figure 7). Like the analysis above (Figure 4), these plots show amplitude values normalized to the mean amplitude of the dataset for each time series. This differed from the calm data set in that wells nearest to surface water (N1, L1, L3, and DL1) showed two of the three dominant periods observed in the surface water signal (24 and 25.8- hours) and the farthest inland wells (N2, N3, M1, M2) showed more focused periodicity at 24-hour interval.

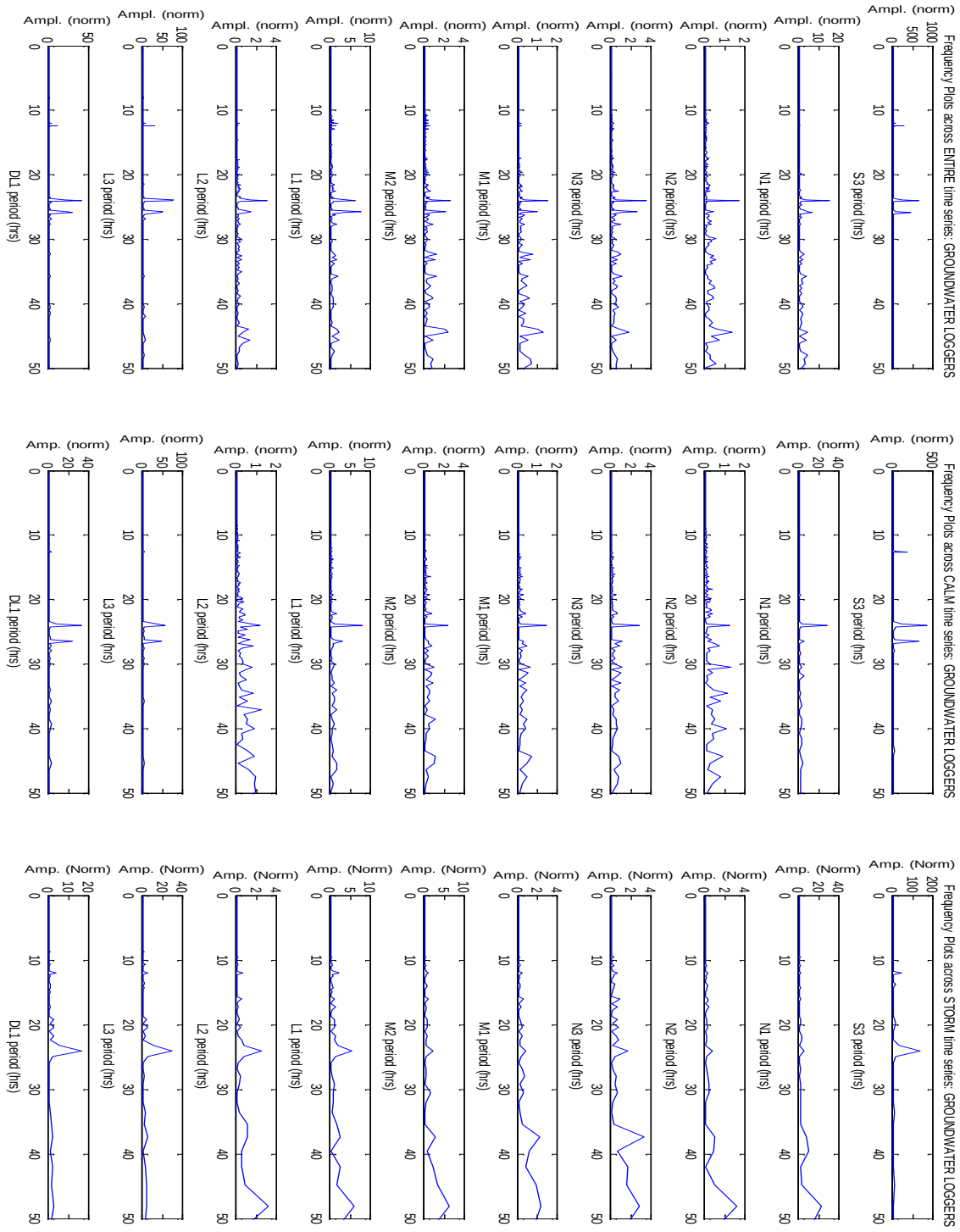

Figure 7: Fourier frequency analysis results for surface water data (row 1) and groundwater data (rows 2-10) for the entire time series (left), the storms time series (center), and the calm time series (right). Response patterns in nearshore wells N1, L1, L2, L3, and DL1 were more similar to surface water in the channel (S3) than were inland wells N2, N3, M1, and M2.

3.2.2 HORIZONTAL GROUNDWATER GRADIENTS

The gradient established between the surface water and piezometers at the island edge (N1, L1, and DL1) fluctuated both during times of storm events and calm periods, as both the surface water and the island edge groundwater were affected by tidal and diurnal fluctuations in water level (Figure 8). Depending on the surface water level near the well locations, flow occurred either into or out of the island. Across the entire calm time series, conditions that created outward flow (toward the main channel, negative in Figure 8, top row) tended to dominate. During storm events, however, gradients almost exclusively directed flow inwards from the channel into the island edge (positive in Figure 8, bottom row).

In the inland portion of the northern island, gradients were relatively stagnant in comparison to the near-channel gradients, but rapid shifts in gradients sometimes occurred, as is seen during the storm week portrayed in Figure 8, bottom row. When undisturbed by storms, the gradients suggested northwards flow from N1 to N2, away from the lagoon and toward the channel. However, storms caused that gradient to lessen or even reverse, causing flow from the apex into the inner island. Immediately following storms that caused island inundation, a pressure 'mound' developed at N2, as flow was directed both north towards the island apex and south towards the island lagoon.

Gradients between the lagoon (L3) and the inner island (N3) were usually extremely low; however, after lengthy periods without storms, small but discernable flow into the island from the lagoon was observed. The mid-island transect showed gradients more dominated by the surface water periodicity. Despite this periodicity, however, groundwater gradients rarely changed across calm times. During storms, there were inward-flowing gradients from both the lagoon and the channel edges of the transect,

causing flow into L1 and L2. As storms receded, the gradients reversed between both L2 and L3 and between L1 and L2, as the inland-directed flow observed during storms became outward-directed flow.

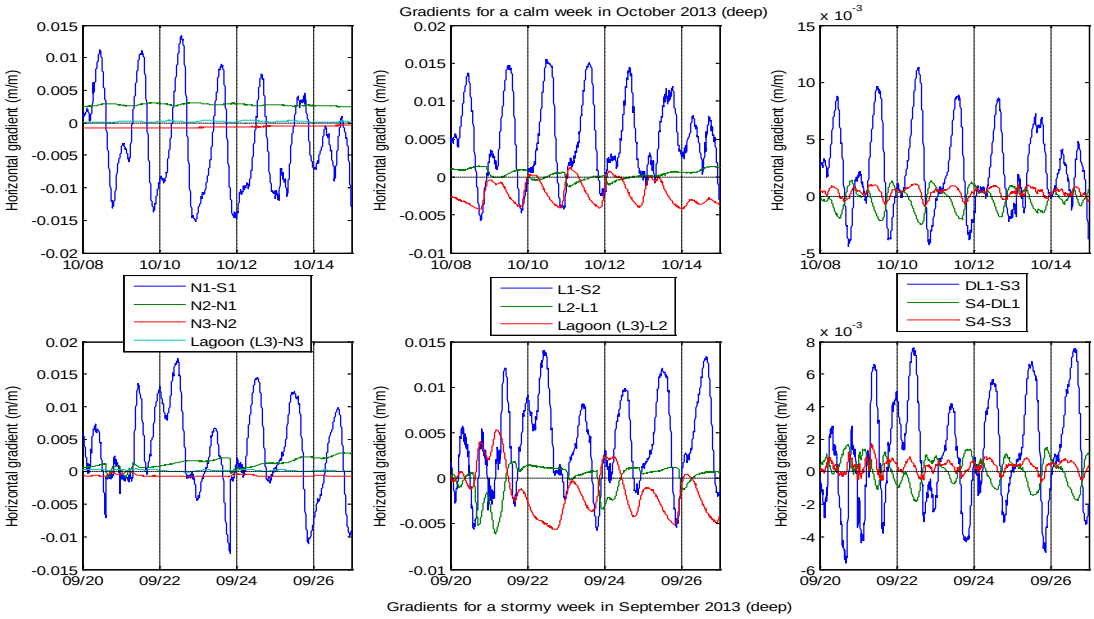

Figure 8: Horizontal gradients between neighboring wells and the nearest surface water logger for each transect during (top row) the calm week between 10/8 and 10/15/2013 and (bottom row) the stormy week between 9/20 and 9/27/13. Positive gradients indicate flow directed into the island from the channel (toward the lagoon); negative gradients, the reverse. In the third column of plots, the S4-S3 gradient indicates the surface water gradient between the distal lagoon (S4) and channel (S3) across the sand bar-like levee hosting well location DL.

The lowest, most distal well cluster (DL1 shallow and deep), which was closely bounded by surface water on both sides, showed gradients that responded to surface water dynamics on a diurnal time scale. During calm times, the system shifted from periods where flow was directed inland from both the lagoon and channel to periods

where flow was directed outward from the sandbar. This shift happened every day. Storms perturbed the periodicity of this pattern, but did not necessarily disturb the pattern itself. However, brief moments also occurred outside of the extent of the presented data when flow was observed unidirectionally, from the either the lagoon surface water (S4) through the sandbar (DL1) and into the channel (S3), or vice versa (see Appendix).

3.2.3 VERTICAL GROUNDWATER GRADIENTS

As mentioned above, the shallow and deep wells within a pairing behaved very similarly in most places (Table 1). In the strongest case of disparity, at pair L2, site and data inspection suggest the deep L2 well screen was clogged and thus the logger was receiving a damped signal. Thus, data from this well were discarded. Additionally, it is likely that sediment collection at the bottom of the shallow N3 well led to artificially disparate data after November 4, 2013, so data collected in that well beyond that point were also omitted from analysis.

Groundwater potentials exceeded local land surface elevation at the majority of locations and for the majority of the study period (Figure 9), however, at no point within the study were they stagnant. The local potentials seemed to follow a constant pattern of flooding and draining, with potentials exceeding ground surface most significantly at times of inundation (e.g., October 8, 2013 (Figure 9)), and potentials receding to their lowest points, in some cases below ground surface, at the longest drainage times (e.g., October 15, 2013 (Figure 9)). Well pair N1 was the only site where groundwater potentials consistently fell below local land surface elevation, yet even in this location, significant inundation events caused the groundwater heads to exceed land surface elevation at these points

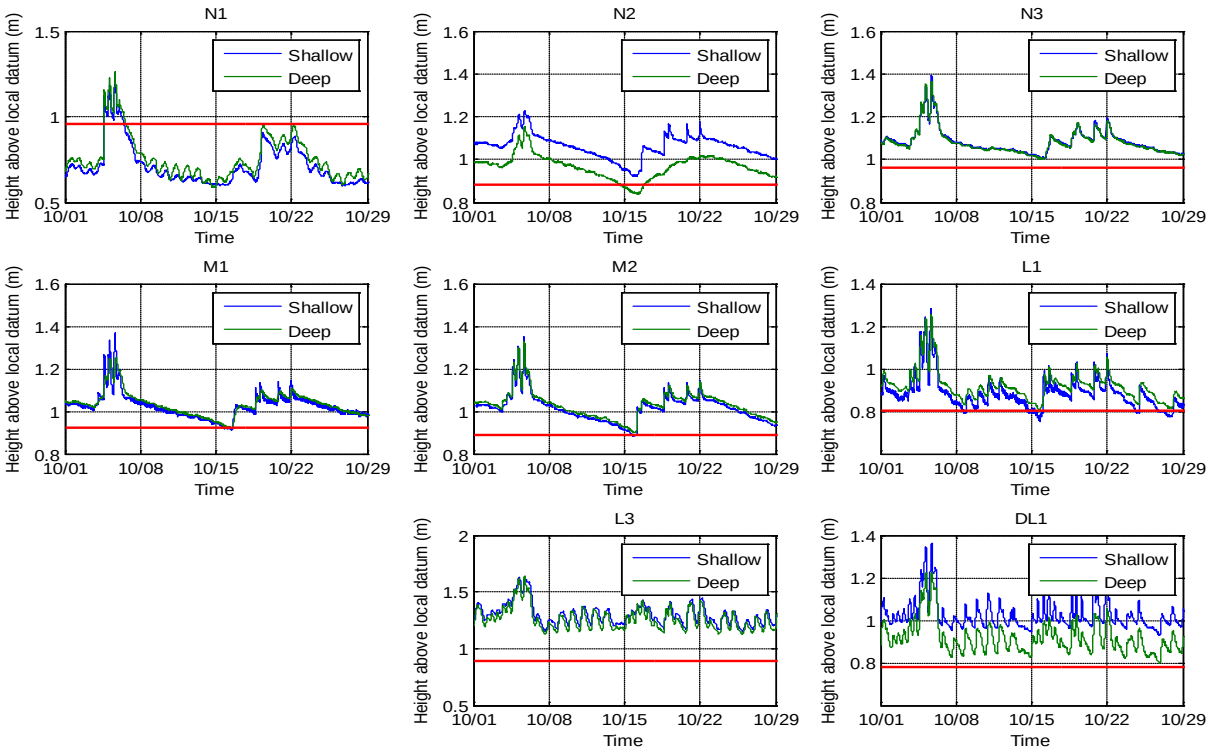

Figure 9: Water levels in shallow (blue) and deep (green) paired wells for October 2013. The vertical datum for each plot is the bottom of the deeper well in each pair. The red line in each plot represents the local ground surface elevation.

Despite the general similarities between shallow and deep well records (Table 2), small vertical gradients did exist at most well-pair locations. The uncertainty inherent in the groundwater head data is anticipated to be about 2 cm due to the resolution of the pressure transducers used, and thus apparent differences less than 4 cm (0.04 m) are ignored.

Under typical (calm) conditions, the largest vertical head gradients occurred at clusters N2 and DL1, both of which exhibited much higher (~10 cm) head values in the shallow well than in the deep well, suggesting downward vertical flow according to a vertical gradient of 10cm/~50cm, or ~0.2. This was also observed at L3, but to a lesser

extent (~5 cm, or ~0.1 cm/cm vertical gradient). The opposite trend was observed at N1 and L1, where upward flow was induced (~8 cm, or ~0.16 cm/cm vertical gradient). Well pairs N3, M1, and M2 showed no discernable vertical gradient within the calm portions of the study period, suggesting hydrostatic equilibrium. Due to the clogged deep well, the vertical gradient could not be identified at L2.

The onset of storm events, such as on 10/8/2013 (Figure 9), influenced the vertical head gradients in the island, but differently in different locations. At well pairs that experienced downward vertical flow during calm periods (N2, L3, DL1) the gradient lessened but flow remained downward. Well pairs that experienced upward vertical flow during calm periods (N1 and L1) did not necessarily maintain it, as diurnal oscillations during the storm event sometimes inverted the vertical gradients. Well pairs that seemed to be in hydrostatic equilibrium (N3, M1, and M2) during calm periods showed slight gradients that would induce flow from shallow to deep during storm events, with the gradient increasing as the storms progressed.

3.2.4 Rate of Rise Analysis

For each storm event, the rate of the potentiometric surface change was calculated for both the rising and falling limbs of the well hydrographs. Each storm event was categorized by a sharp and rapid rise in groundwater head, followed by a long, constant falling limb. Across all wells within the upper (N) and middle (M) transects, the average rate of potentiometric surface decline was 3 cm/hr for the extent of the falling limb. Lower-island well hydrographs (L, DL) were omitted from this analysis because they were more strongly influenced by surface water fluctuations during both calm and stormy days (see Fourier analysis and regression results), and thus an analysis of hydrograph rise

at these locations would not sufficiently isolate a storm-event groundwater activity from calm-event groundwater activity.

Well N1 showed the fastest average rate of rise overall, an order of magnitude greater than the other four wells analyzed (Table 3). However, it should be noted that the mean for well N1 was skewed by extreme storm events on and around 9/23, 10/6, 10/31, and 11/17, which disproportionally affected it more than the other wells and resulted in rates of rise of 0.199, 0.226, 0.239, 0.252 m/h, respectively. These rapid rises in hydraulic head were well outside the standard deviation of Well N1 rates. These instances also coincided with the highest surface water levels observed in the study period, which raised the groundwater head at N1 above the ground surface elevation.

	N1	N2	N3	M1	M2
Mean (m/h):	0.112	0.017	0.023	0.014	0.028
Standard Dev. (m/h):	0.076	0.012	0.016	0.009	0.018
Median (m/h):	0.090	0.013	0.018	0.013	0.024
Minimum (m/h):	0.008	0.001	0.002	0.003	0.005
Maximum (m/h):	**0.252**	0.046	0.078	0.040	0.073

Table 3: Summary of rate of rise analysis for N- and M- transect deep wells during the rising limb of wells' storm hydrographs.

4. Discussion

4.1 Overall Pintail Island hydrologic structure and dynamics

According to the results obtained during the study period (9/9/2013 to 2/4/2014), the surface water hydrology surrounding Pintail Island was dominated by tidal signals and diurnal wind signals that caused water level fluctuations ranging from 20 cm to over 1 m. Even small changes in surface water levels greatly affected inundation patterns of the system as the entire relief of the island was only about 50 cm. This was not independent of island morphology, however. The subaerial island elevation distribution appeared to be bimodal rather than gradated (Smith, 2014; NCALM, 2009). The 'southern' zone (Figure 5) fell below a topographic scarp observed in the field and encompassed the newer island limbs and lagoon that were frequently inundated. The groundwater head data from the two well pairs in this zone, L3 and DL1, were closely related to diurnal and tidal surface water signals, and exhibited only slight lag. The 'northern' zone of the island sat atop a cut bank and was rarely overtopped by high surface water levels, as reflected in the remainder of the wells (M and N transects), which did not exhibit responses to diurnal and tidal surface water fluctuations during calm weather periods. Landsat imagery of the island also showed inundation of this northern zone to be a rare occurrence (Smith, 2014). The hydrogeologic structure of the island differed between the northern and southern zones and this difference greatly affected the groundwater dynamics of each. Previous literature has well established that groundwater signals within islands are often a damped reflection of surrounding surface water signals, and the amount of damping that occurs can depend on the distance of the signal from the surface water boundary and the permeability of the intervening porous medium.

The rate of change of groundwater head values within wells can provide insight into surface inundation conditions, and this information helped categorize the island zonation defined above. In saturated, flooded systems not far distant from hydrostatic equilibrium, changes in surface pressure are directly reflected at depth, so changes in flooding surface water levels would be reflected in groundwater records. There were brief moments on and around 9/23, 10/6, 10/31, and 11/17 when even the northern zone experienced groundwater head changes at abnormally fast rates, at times corresponding to heights in surface water. The typical groundwater rise from storm events in this zone was 0.005 to 0.04 m/hour (Table 3), but the four extreme events listed above drove the rate of rise at both N1 deep and shallow wells to exceed 20 cm/hour, which suggests a different process causing the rise at these times. It is likely that the piezometers installed at site N1 were not sealed as well as the others and so were subject to preferential vertical flow from the surface. This annulus flooding could explain the rate of rise anomalies during times when the surface was flooded. This was not observed at any other point in any other N or M transect well throughout the study, which either suggests that no other well cluster experienced annulus flooding or that this zone did not experience inundation during the study period.

The Fourier Frequency analysis identified dominant periodicity within the system during calm times, which suggested that, when undisturbed, the system was strongly periodic. These dominant periods were at 12.5, 24, and 25.8 hours. Further Fourier analysis of environmental factors indicated that likely sources of these periodicities were tidal energies, which were maximal at 12.5 and 25.8 hour intervals, and the wind speed energy, which was maximal at 24 hours. This analysis supports, Geleyense et al. (2014) who identified wind as a dominant factor in water level fluctuations in this system. The

same Frequency analysis showed that storm events exhibited very little of the predictability observed in the rest of the period of record. During these times, the tidally-attributed periodicities disappeared completely, and the wind-driven periodicity became much more diffuse, suggesting higher variability in the timing of wind and rain during storm events. Storm events bring high winds and heavy rains, which influenced and amplified precipitation and wind speed but left the lunar tide unaltered. Thus, the tidal influence appeared to become overwhelmed by much larger surface water fluctuations driven by wind and rain. Because of the stochastic nature of the storm occurrences, the dominant periods were not precise. This difference between calm- and stormy-period responses was also seen in the groundwater signals, which showed single, diffuse diurnal peaks rather than tidal peaks throughout storm events (Figure 7).

4.2 NORTHERN ISLAND 'CONFINED' GROUNDWATER ZONE

Field observations showed a 'fining up' of grain size distribution in the northern zone; Smith (2014) also reported this. The fine surficial sediments were of low hydraulic conductivity (0.2 cm/day, Hyprop data, Appendix), which acted as a confining layer on top of this zone. This allowed for the island surface environment to be apparently hydrologically disconnected from its shallow subsurface. Thus, the northern island subsurface could viably behave like a semi-confined aquifer, maintaining pressure heads that exceeded the ground surface for long periods beyond inundation events (Figure 9).

Because of the steep and tall cut bank on the outer channel edge of the island, the coarser sediment underlying the shallow, low-conductivity cap was in direct contact with channel and lagoon water; thus, most water and pressure inputs and in this semi-confined

zone must be laterally driven. The results of the horizontal gradient analysis showed that mild storm events caused groundwater gradients to be directed inland from the channel surface water into the island groundwater. Because the island was saturated during the extent of the study, it is unlikely that significant flow occurred from the surrounding surface water into the groundwater. However, these storm events created pressure pulses that propagated laterally toward the center of the island, impacting groundwater levels, which manifested as the initial pressure spike observed in the inland piezometers during storms. Following this initial pulse, horizontal gradients show that the island groundwater depressurizes relatively constantly, but the gradient direction changes (e.g., toward the channel or toward the lagoon). During the study, we observed periods when depressurization occurred to both sides, and other periods when depressurization only towards the apex. This variable behavior was contingent on the boundary conditions (surface water conditions) that existed at the lagoon and the channel—if lagoon water elevation exceeds channel water elevation, drainage should occur toward the apex only. Otherwise, gradients could exist in either direction. During the largest storms, the island was over-topped and the typically dominant lateral boundary conditions were trumped by the imposed overlying boundary condition of a surface flood. Here, the pressure pulse being delivered to the subsurface surrounded the entire system.

The vertical gradient analysis showed that, in general, little vertical flow occurred in the system. Head differences measured between most wells within a well pair were near the margin of uncertainty (estimated to be 4 cm). However, in the cases of wells N1 and L1, significant upward vertical gradients were observed. These wells were located in the thin outer levee of the island, and both were in the middle of black willow (*Salix nigra*) groves at the highest elevation found on the island and likely the region where the

layer of fine material is thickest (40-50 cm). Thus, this may be the only region of the island where semi-confined behavior was fully captured, as the higher-permeability deeper sand layer accessed by the deeper wells was hydrologically well connected to the nearby channel, allowing for relatively rapid propagation of pressure pulses within the layer. The lower-permeability shallow clay layer accessed by the shallower wells, being hydrologically disconnected and less frequently inundated, did not readily experience these same pressure pulses. Because the deep wells responded to diurnal surface water changes, groundwater became hydrologically overpressured with respect to the shallow layer when surface water rises. This was illustrated in well pairs N1 and L1 (Figure 9), where a diurnal pattern of alternatively increasing and decreasing gradient was observed between the shallow and deep wells, from levels that fell within total head uncertainty to levels that exceed it. This was not observed at other well pairs, possibly because pressure pulses do not reach the other well locations in the middle of the island, unless a storm inundates the system. Another explanation is that the shallow wells at other locations might have been completed below the confining layer; thus both the deep and shallow wells recorded the same confined behavior.

N1 was the only well pair that consistently showed groundwater heads below ground surface. The lack of artesian pressure at this location, despite being semi-confined, could be explained by its proximity to the channel and was thus the first site to depressurize following a storm event. Additionally, it was the most heavily vegetated location among those included in the study and thus could have been losing the most water to plant transpiration.

4.3 SOUTHERN ISLAND 'UNCONFINED' GROUNDWATER ZONE

The southern zone was characterized by larger median grain sizes, as was determined through field observations and similarly reported by Smith (2014). It was lacking a fine-grained sediment cap, and behaved as an often-inundated, saturated, unconfined aquifer that was fully connected to the surface water surrounding it. A lag of roughly one hour existed between the water levels in the inner lagoon and outer channel, and that lag set up horizontal hydraulic gradients through the sandy island limb on which DL1 was situated (Figure 8). The horizontal gradients showed relatively frequent shifts in the magnitude and direction of the gradient within this sandbar-like island levee, suggesting that this location could be experiencing relatively rapid surface water/groundwater exchange. From a biogeochemical perspective, the relatively high flow in this zone could allow for dissolved organic carbon concentrations to remain sufficiently high for the denitrification of nitrate-rich surface water in zones beneath the surficial oxygenated sediments (Musslewhite et al., 2003).

5. Conclusions

The results of this study indicate that the groundwater hydrology of Pintail Island is spatially-variable, transitioning from a semi-confined older northern island zone to an unconfined, younger southern island zone. The confined zone of the island is able to maintain piezometric head levels that exceed ground surface for long periods of our study. The elevated head levels are established through infrequent, stochastic floods driven by wind and precipitation events and are retained because of a combination of factors: the confining layer that overlies the aquifer system disconnects groundwater from the flood water just above it. Low horizontal gradients lead to a slow draining process. This confined zone is not responsive to the diurnal fluctuations of surface water observed within the surrounding island channel and lagoon unless perturbed by a storm event, at which point, the entire island subsurface responds to surface water fluctuations. The near-channel portion of the island levee is an exception to this rule, where groundwater is more responsive to surface water fluctuations; however, the response is both damped and lagged.

The hydrodynamics of the southern zone of the island depends strongly on the surface water forcings surrounding it. This zone is also frequently inundated, as it is the lower-elevation portion of the island that is still most actively prograding. Flow through this sand bar-like limb of the island can experience in-out pumping patterns, as well as flow-through patterns directed either way across the bar, influenced by the lag in surface water levels between the lagoon and channel.

These findings help guide our understanding the hydrologic and nutrient budgets of Wax Lake Delta in general. The other islands, with similar formation processes and thus similar sedimentologies should be expected to have regimes similar to Pintail Island

studied herein. Knowledge gained in this study could help constrain water budget and nutrient budget estimates throughout the Delta. As mentioned in the introduction, the continental runoff received at Wax Lake Delta has elevated nutrient concentrations, and thus the potential exists for biogeochemical processing of these nutrients within the subsurface. Knowing the magnitude and directions of groundwater flow (e.g., more rapidly in the southern zone than the northern zone) could help guide where biogeochemical investigations should be targeted, and explain the mechanisms necessary for ecosystem survival. Finally, as Wax Lake Delta is a model system for dynamics and progradation of mixed-grain size coastal deltas in general, the conceptual model developed by this study, the first of its kind for the aquifer of a young coastal delta, may provide a starting hypothesis for investigating other systems more broadly, worldwide.

6. Appendix

Surface Water Linear Correlations to Environmental Data		
	Calm	**Storm**
Tides	0.71	0.75
Wind Speed	-0.34	0.03
Precipitation	0.01	0.05
Atchafalaya Discharge	-0.17	-0.2

Figure 1A: Linear correlations between the 'channel signal' (S3) and environmental factors for the calm and stormy datasets

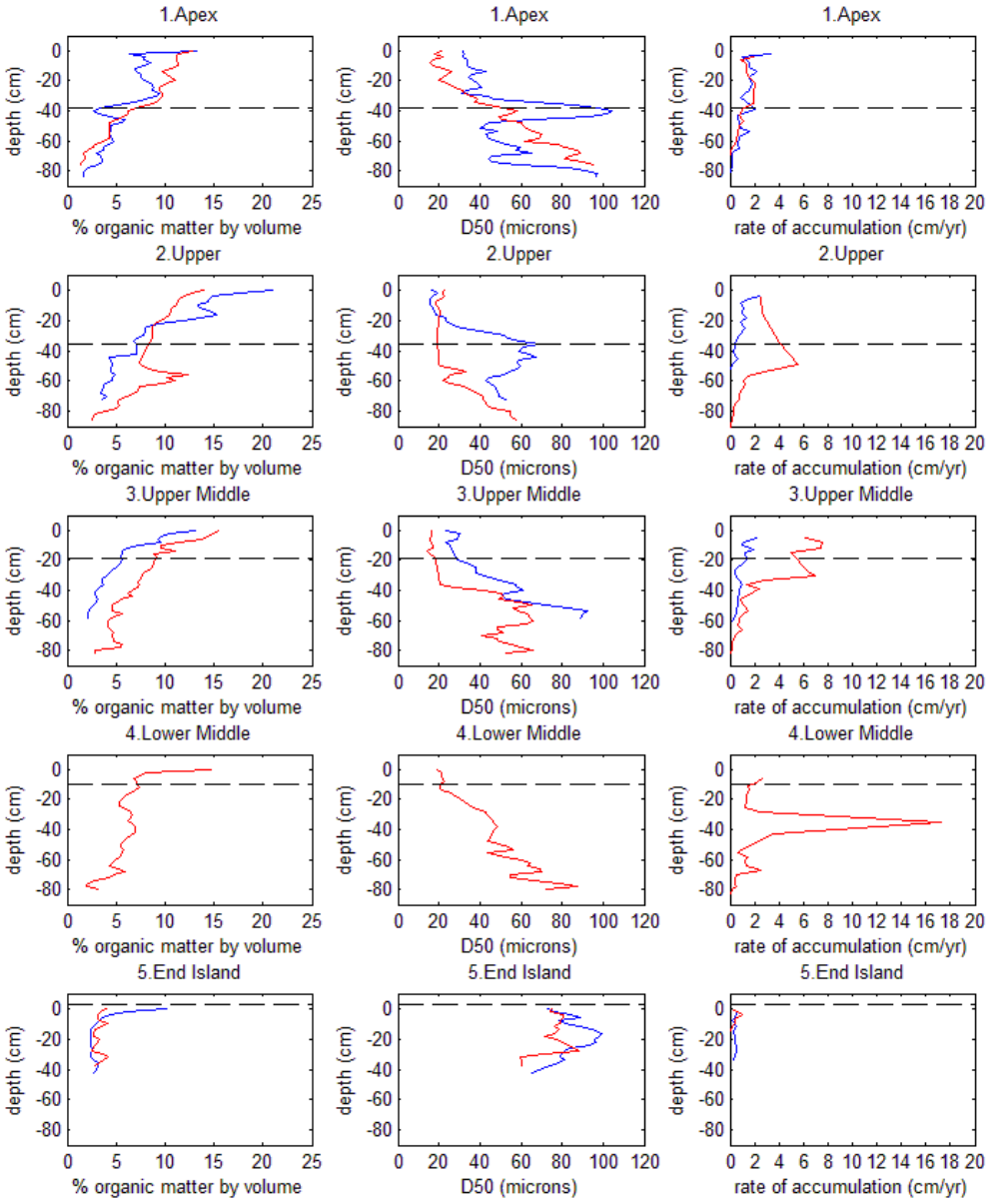

Figure 2A: Summary of core data from Smith et al. (2014). Dotted black line is mean local water level for each site. Each row is one site. Column 1 shows organic matter by volume, Column 2 shows D50 grain size, and Column 3 shows sediment accumulation rates.

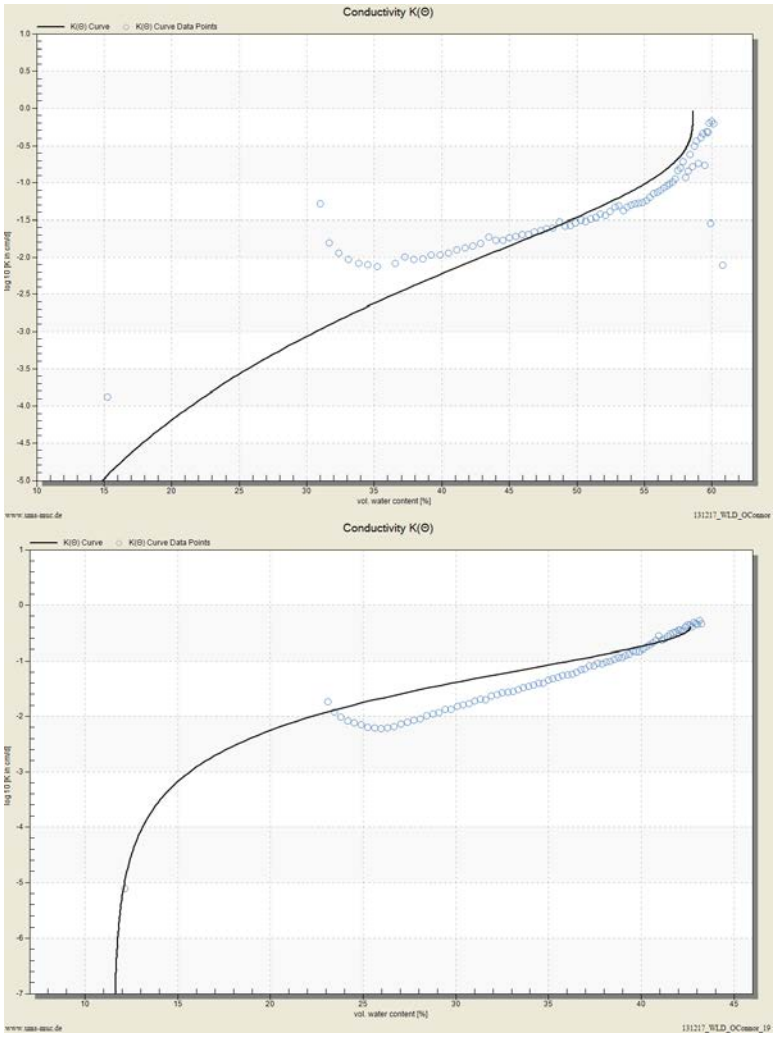

Figure 3A: Averaged conductivity vs. water content plots derived from Hyprop analyses for shallow (top) and deep (bottom) soil samples

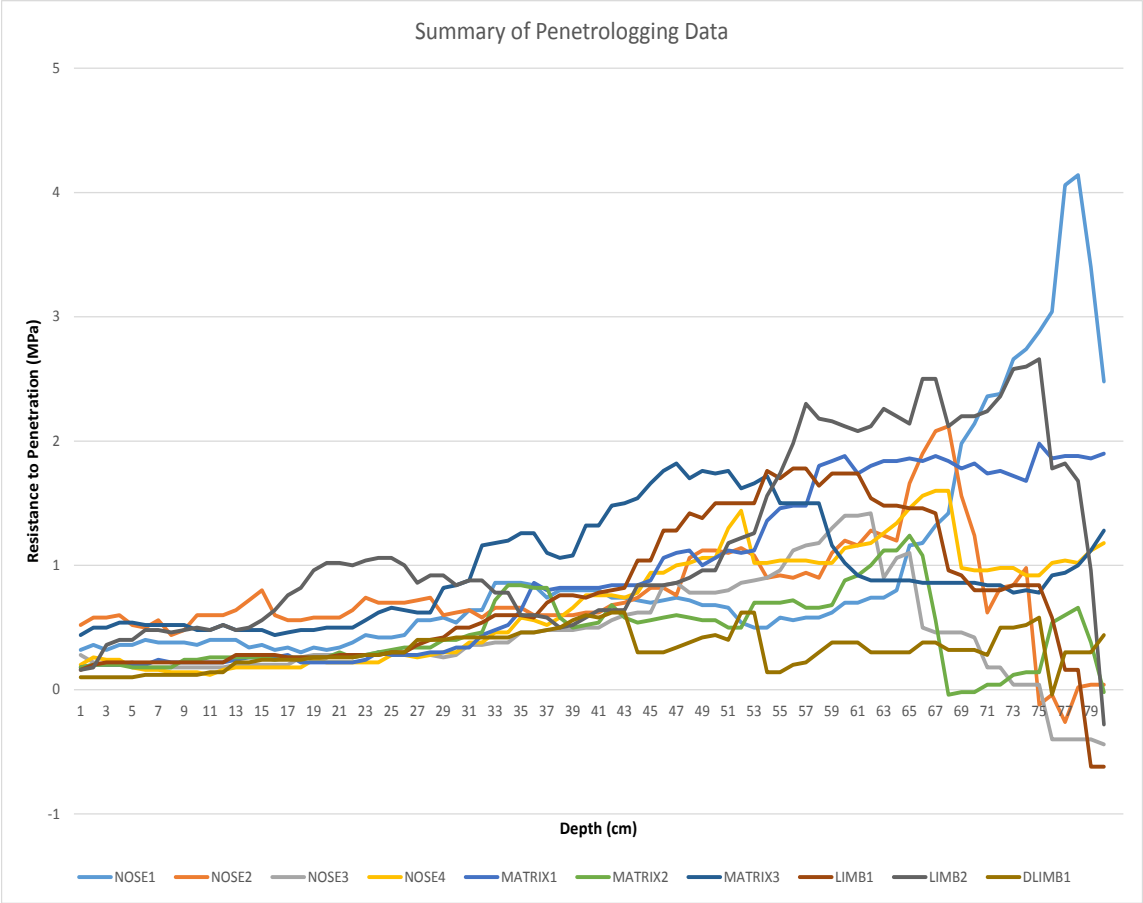

Figure 4A: Penetrologger results for each site. Each line represents the average of five trials at each site

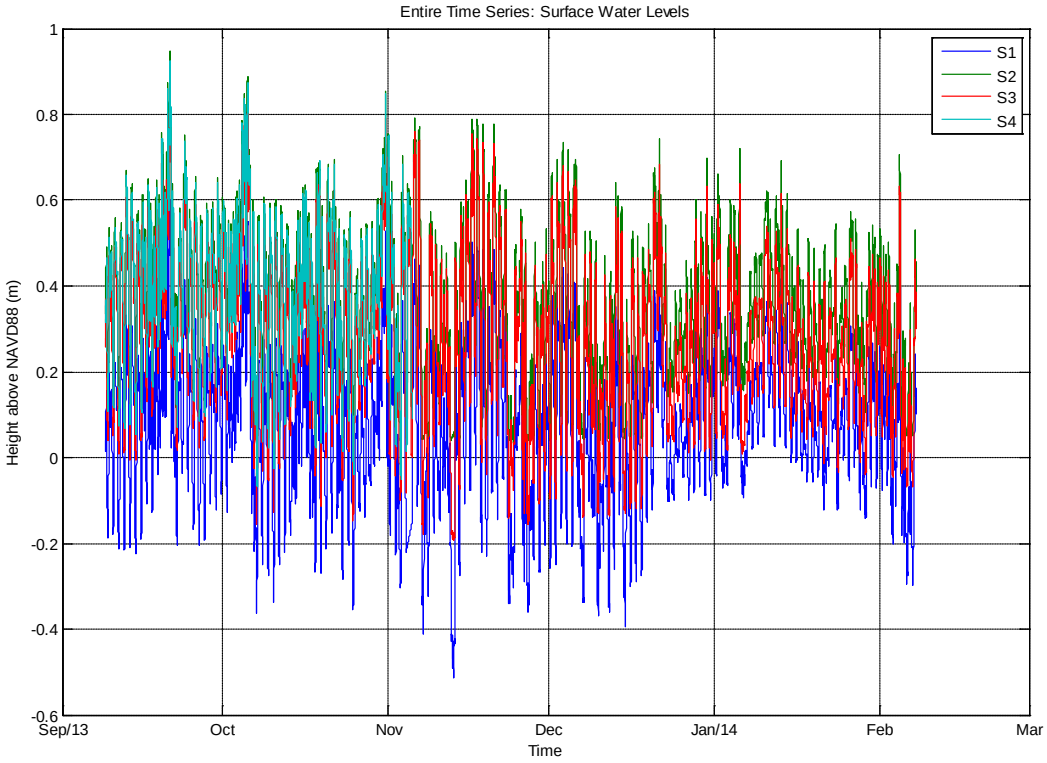

Figure 5A: Surface water levels for the extent of the study. Logger S4 was lost to sea following the November data collection trip.

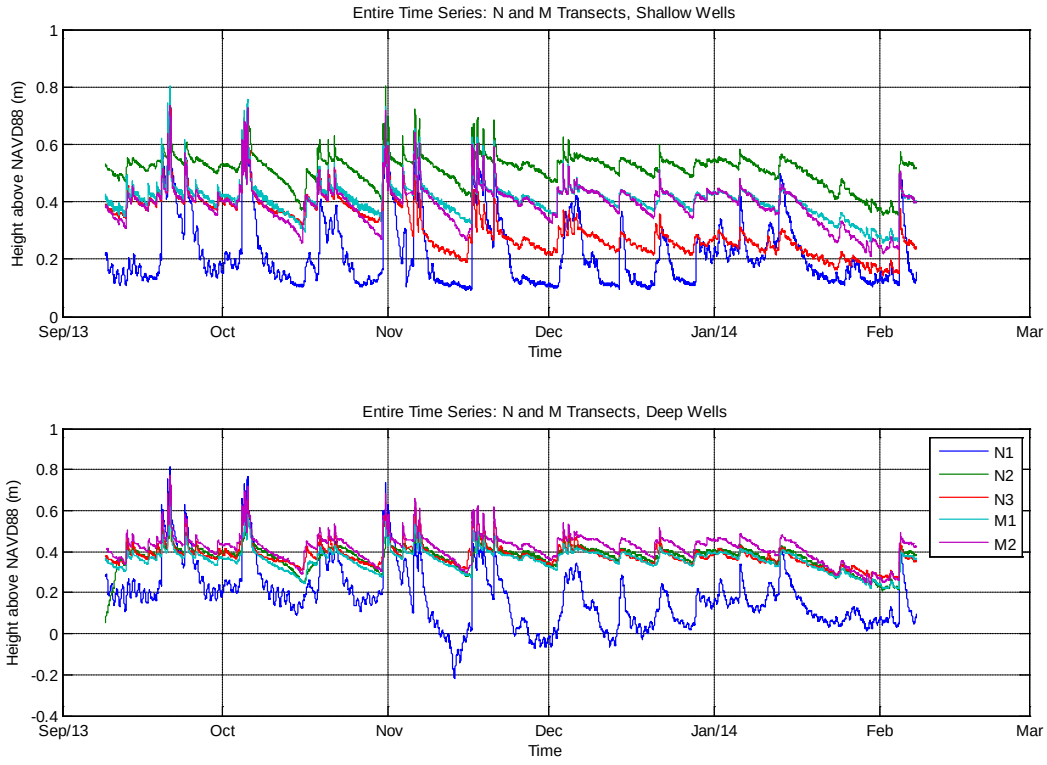

Figure 6A: Groundwater levels across the entire study for the farthest up-island wells (N and M transects)

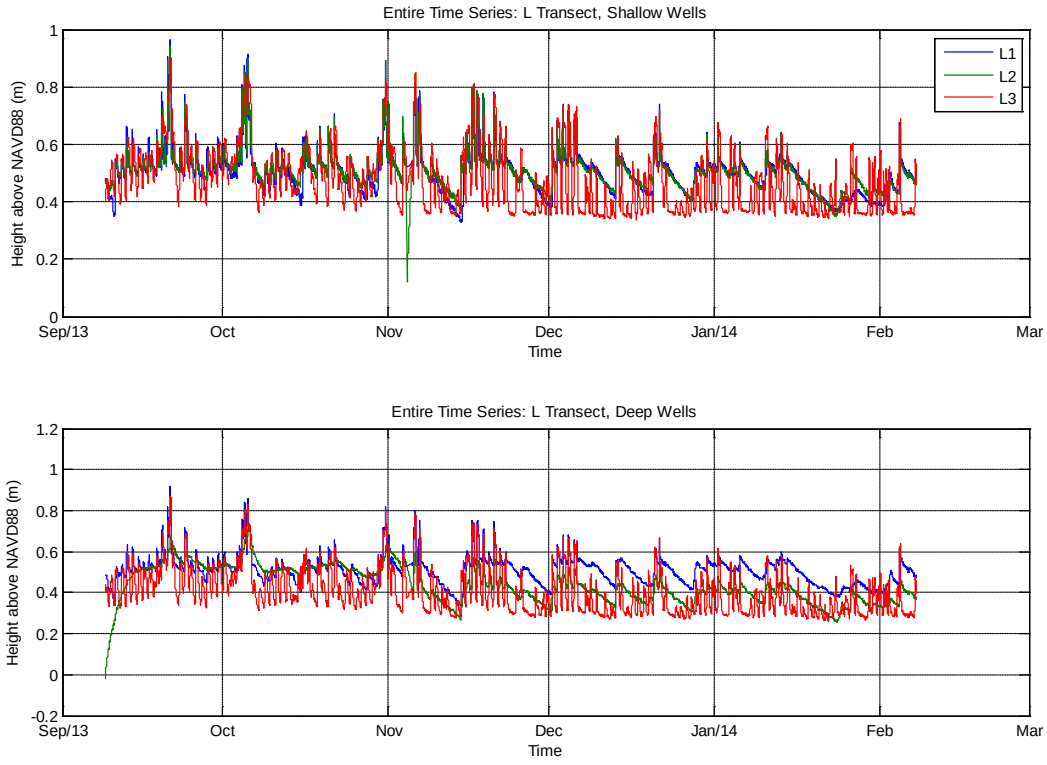

Figure 7A: Groundwater levels observed throughout the study for the middle-island wells ('L' transect)

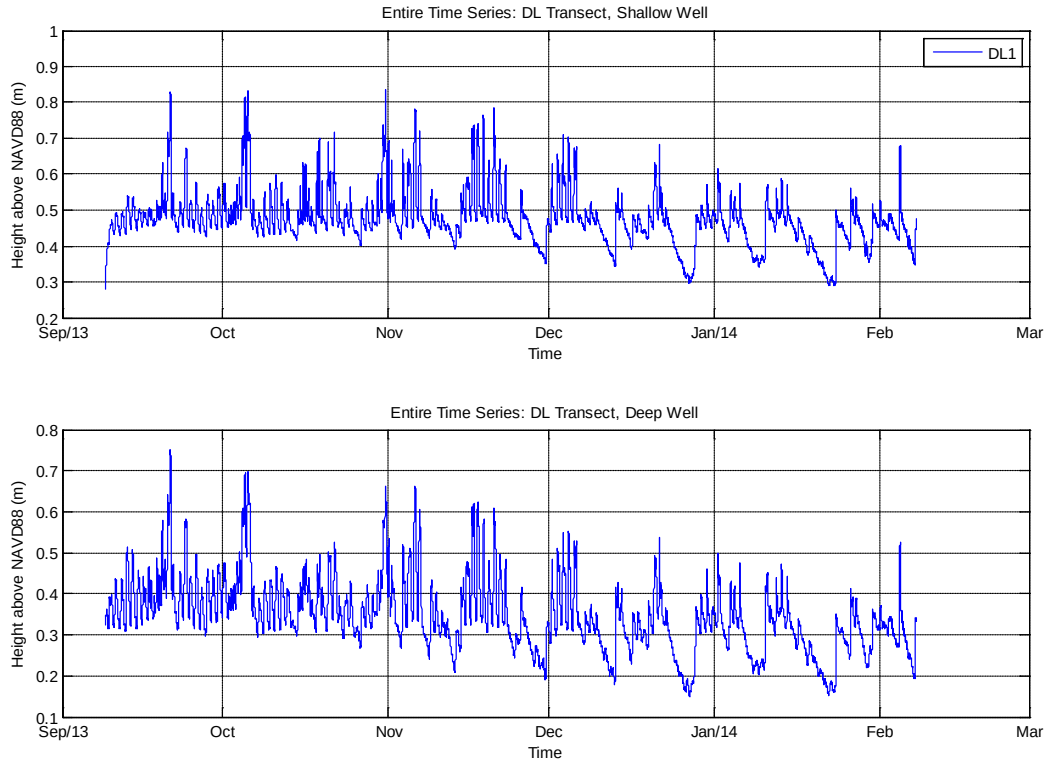

Figure 8A: Groundwater levels observed at the down-island wells (DL transect)

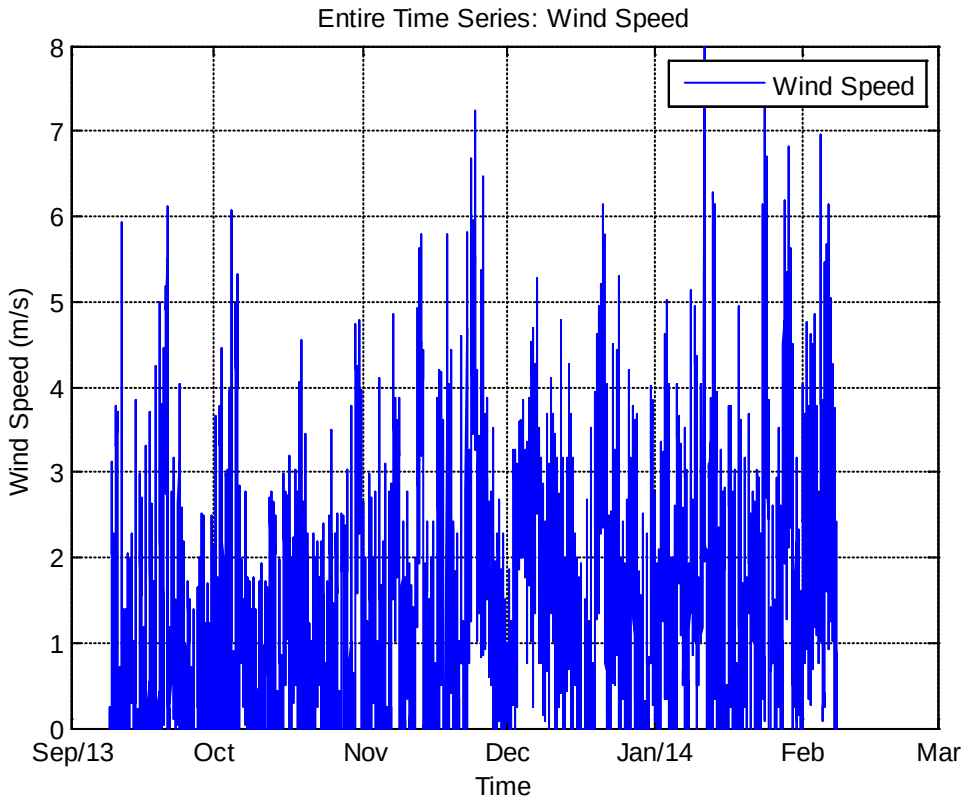

Figure 9A: Wind speed measurements observed at the weather station installed on the apex of Pintail Island

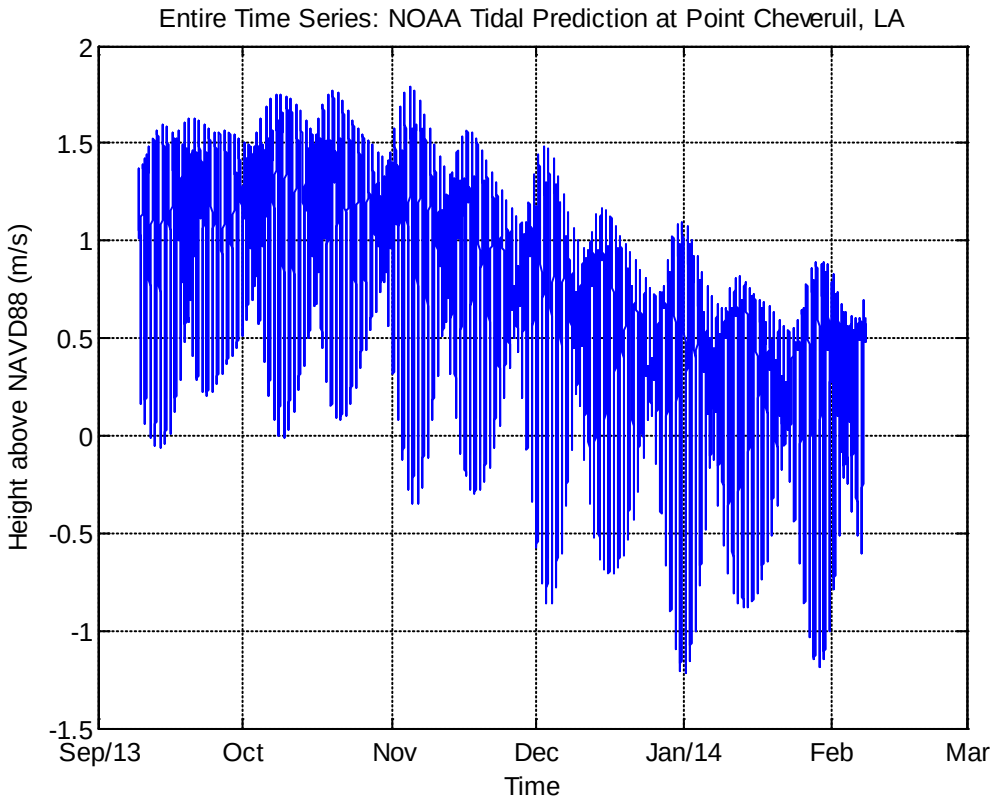

Figure 10A: Tidal fluctuations as predicted by NOAA for Point Cheveruil, LA (8 miles due east of Pintail Island apex)

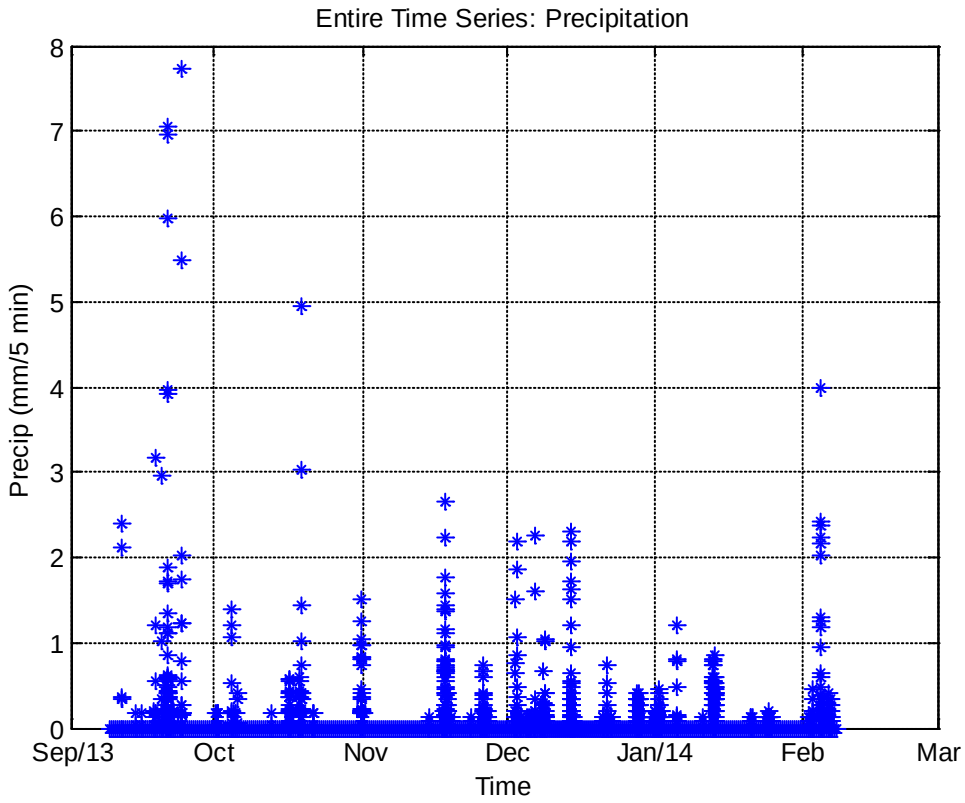

Figure 11A: Precipitation measurements collected at 5-minute intervals by the weather station on Pintail Island apex

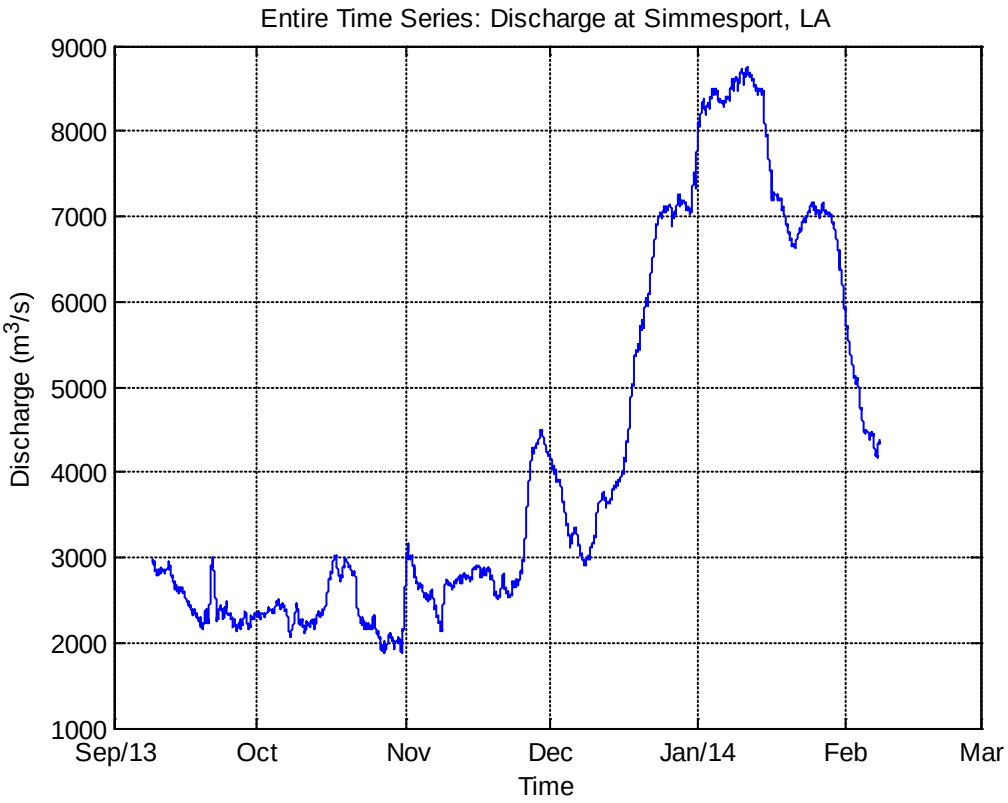

Figure 12A: Discharge measurements reported by the USGS for the gage station in Simmesport, LA for the extent of the study

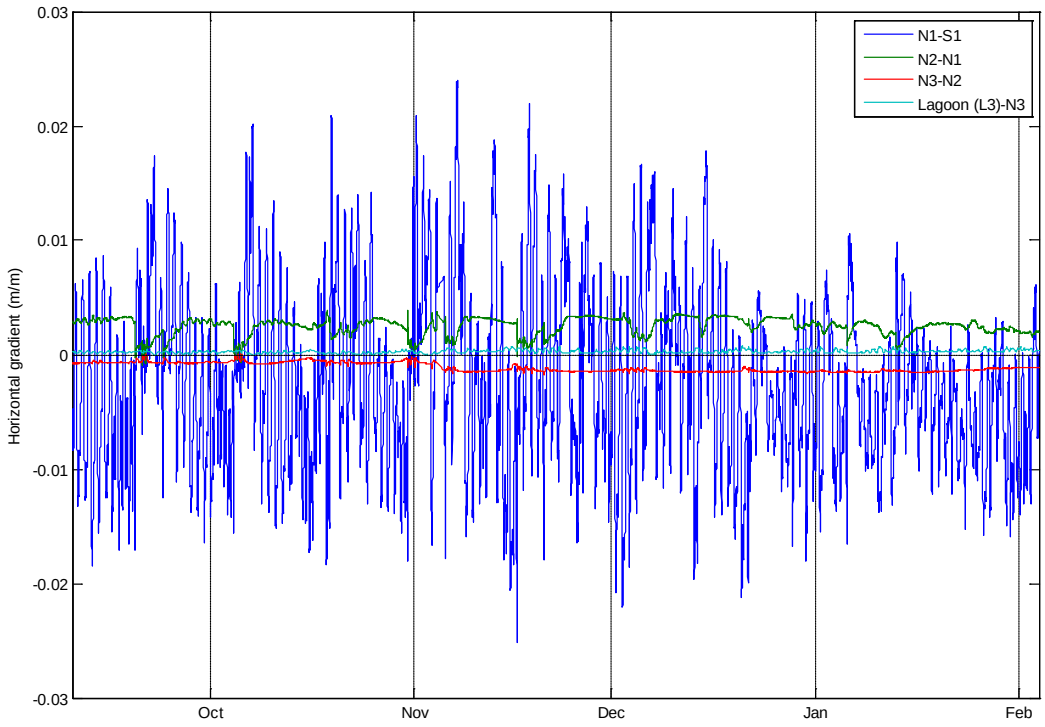

Figure 13A: Horizontal gradients calculated across the entire time of the study for N and M transect wells

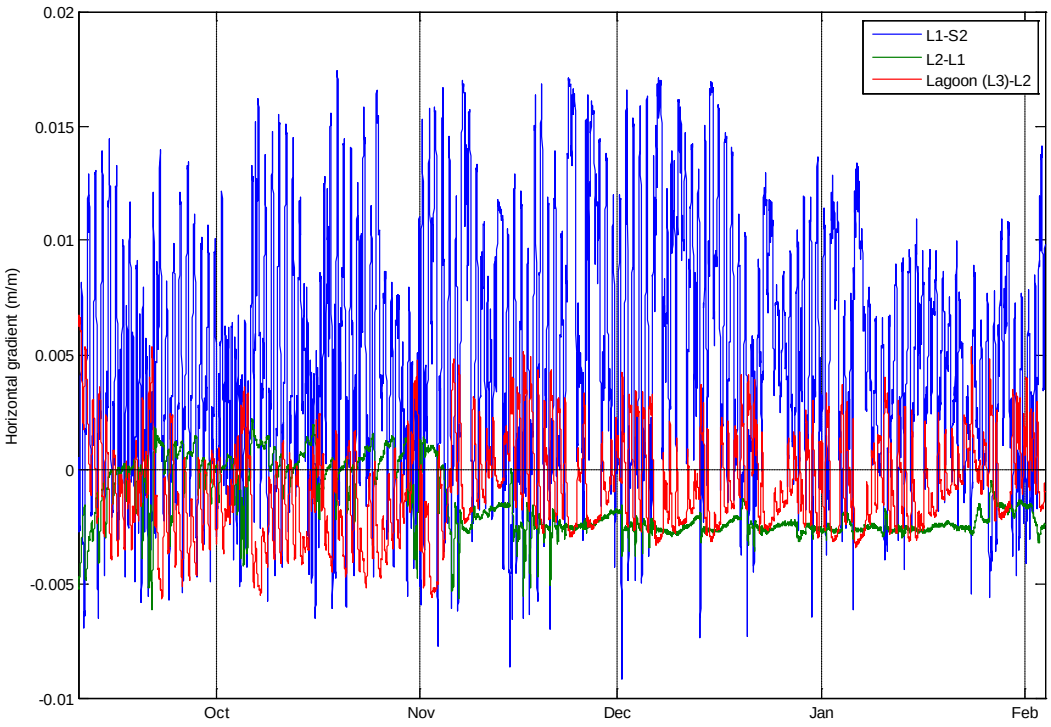

Figure 14: Horizontal head gradients calculated for wells within the L transect for the extent of the study period

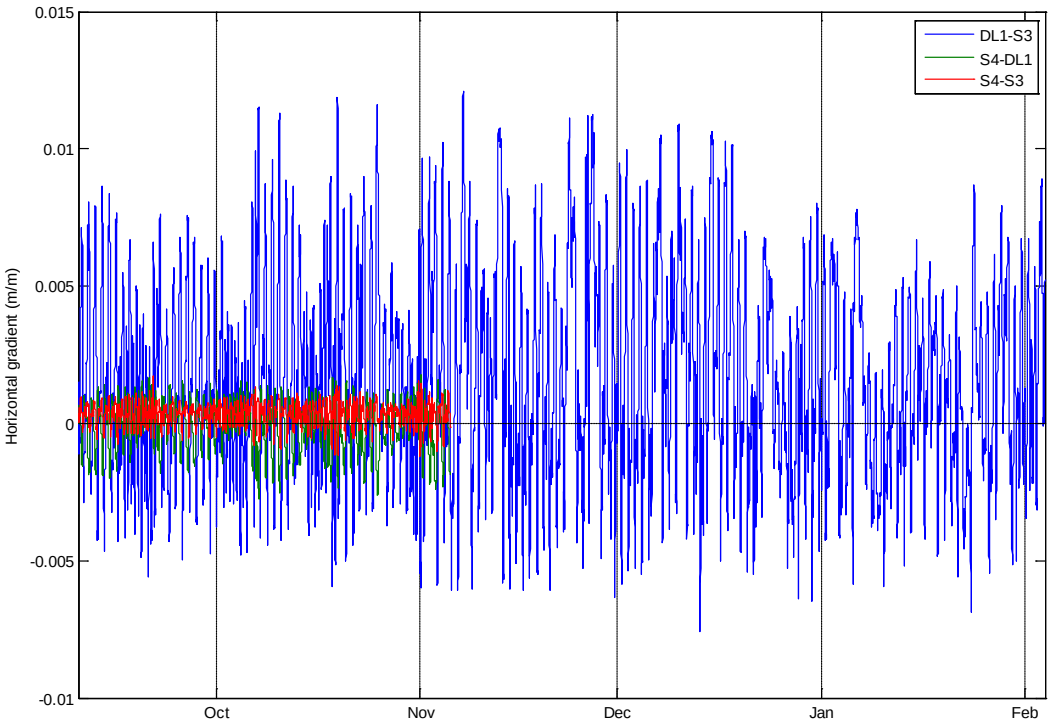

Figure 15A: Horizontal head gradients calculated for wells within the DL transect for the entirety of the study period. No gradients between S4 and either S3 or DL1 were calculated past November 4, 2013 because logger S4 was lost to sea

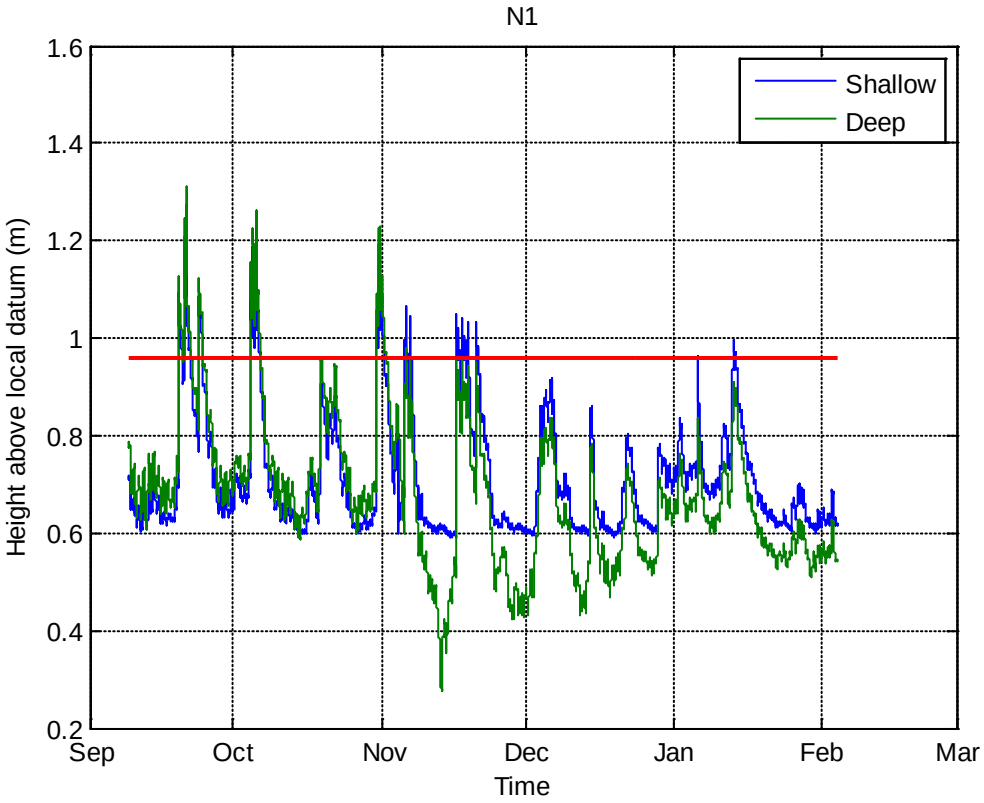

Figure 16A-24A: Head values observed within the shallow and deep wells within each well cluster throughout the entirety of the study period, locally surveyed to the bottom of each deep well. The solid red line represents local ground surface. Plots are organized north to south by transect and numerically within transects.

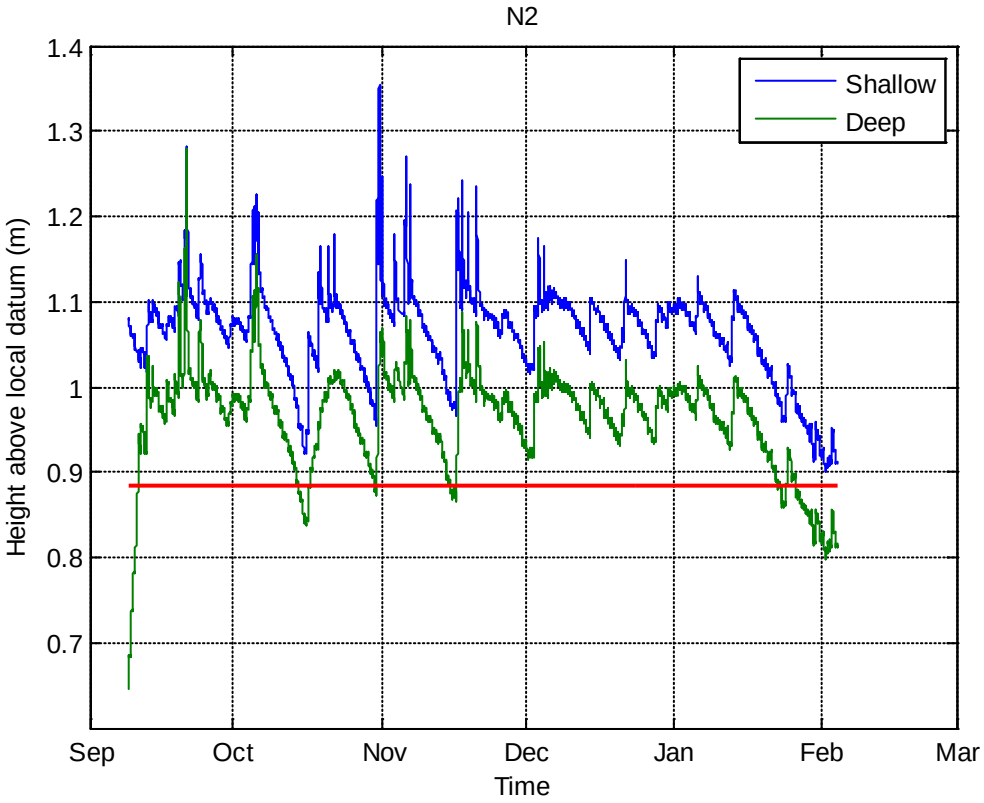
N2
Shallow
Deep
Height above local datum (m)
1.4
1.3
1.2
1.1
1
0.9
0.8
0.7
Sep
Oct
Nov
Dec
Jan
Feb
Mar
Time

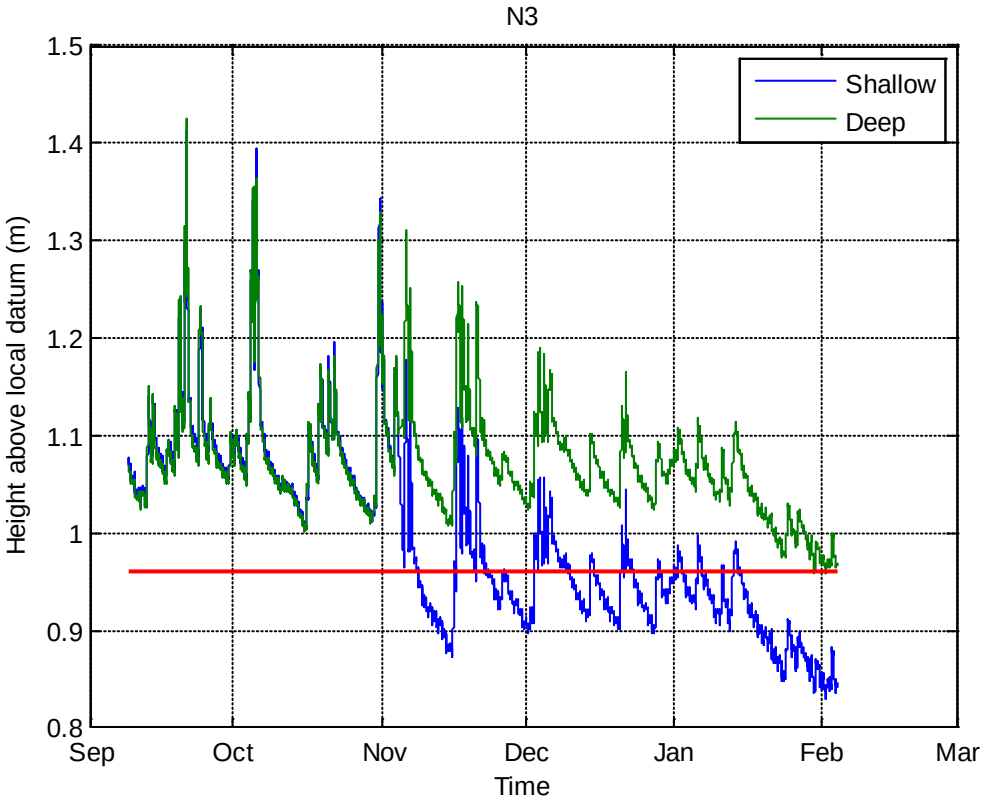
N3
Shallow
Deep
Height above local datum (m)
1.5
1.4
1.3
1.2
1.1
1
0.9
0.8
Sep
Oct
Nov
Dec
Jan
Feb
Mar
Time

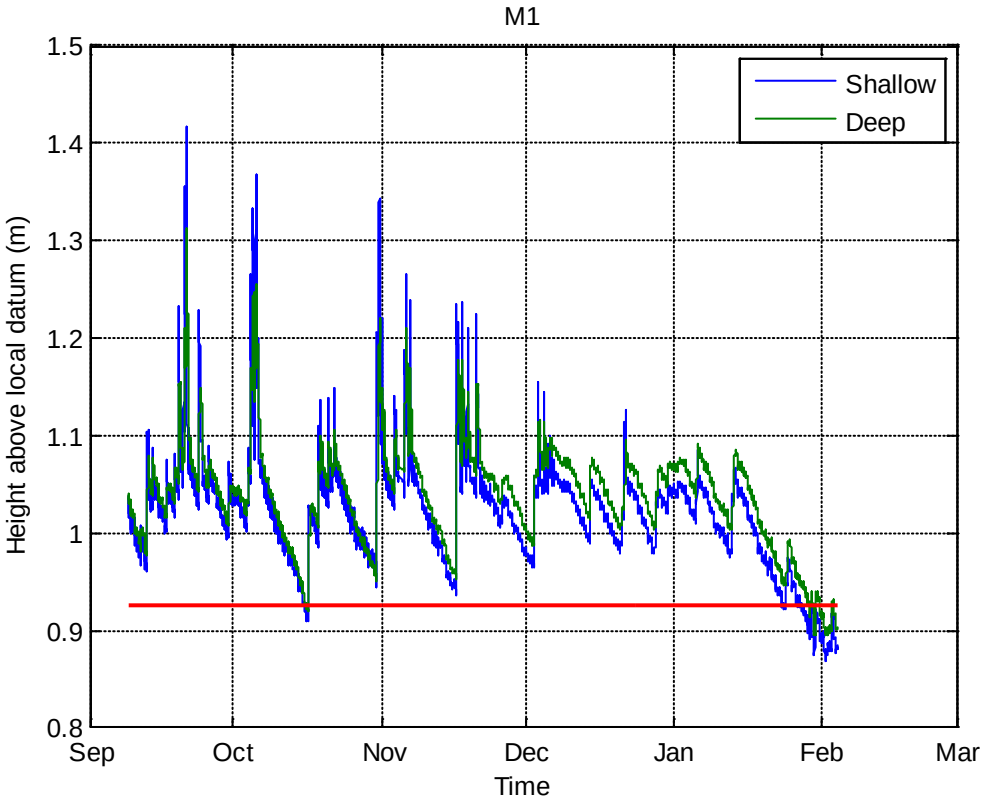
M1
Shallow
Deep
Height above local datum (m)
1.5
1.4
1.3
1.2
1.1
1
0.9
0.8
Sep
Oct
Nov
Dec
Jan
Feb
Mar
Time

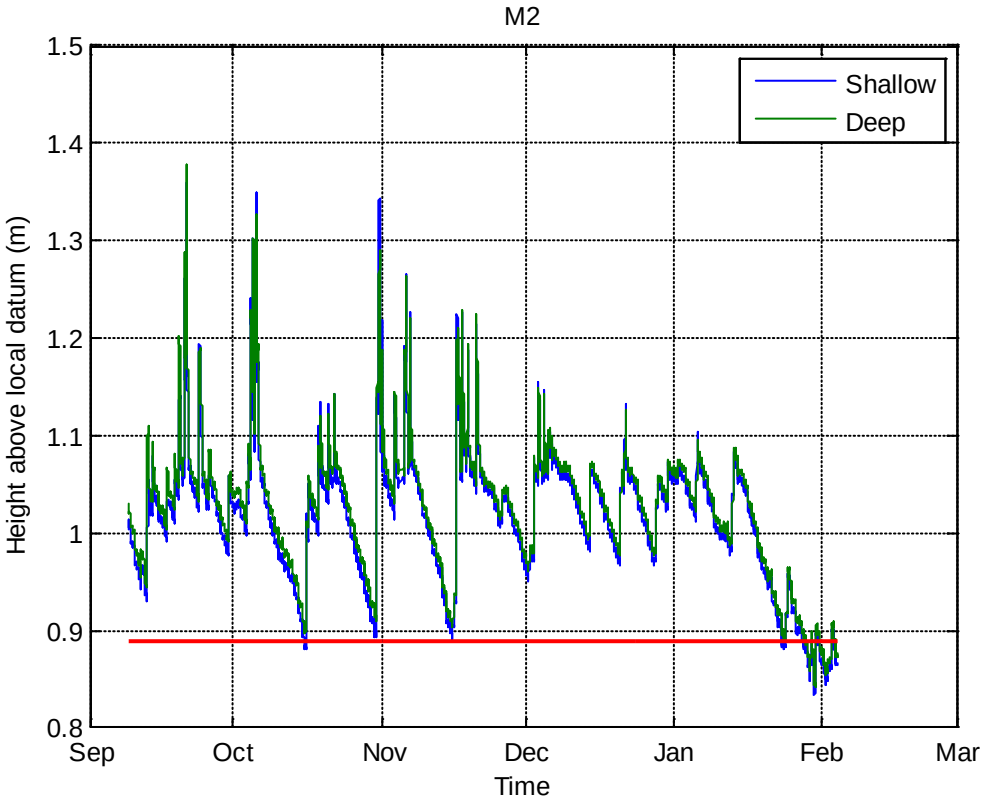
M2
Shallow
Deep
Height above local datum (m)
1.5
1.4
1.3
1.2
1.1
1
0.9
0.8
Sep
Oct
Nov
Dec
Jan
Feb
Mar
Time

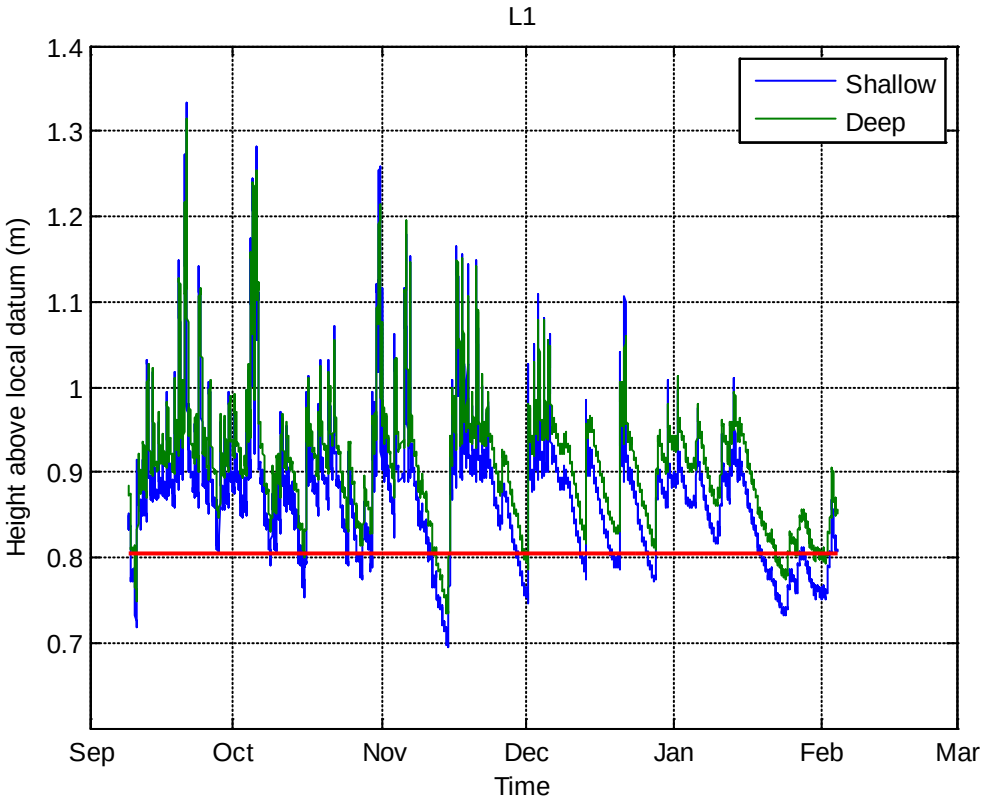
L1
Shallow
Deep
Height above local datum (m)
1.4
1.3
1.2
1.1
1
0.9
0.8
0.7
Sep
Oct
Nov
Dec
Jan
Feb
Mar
Time

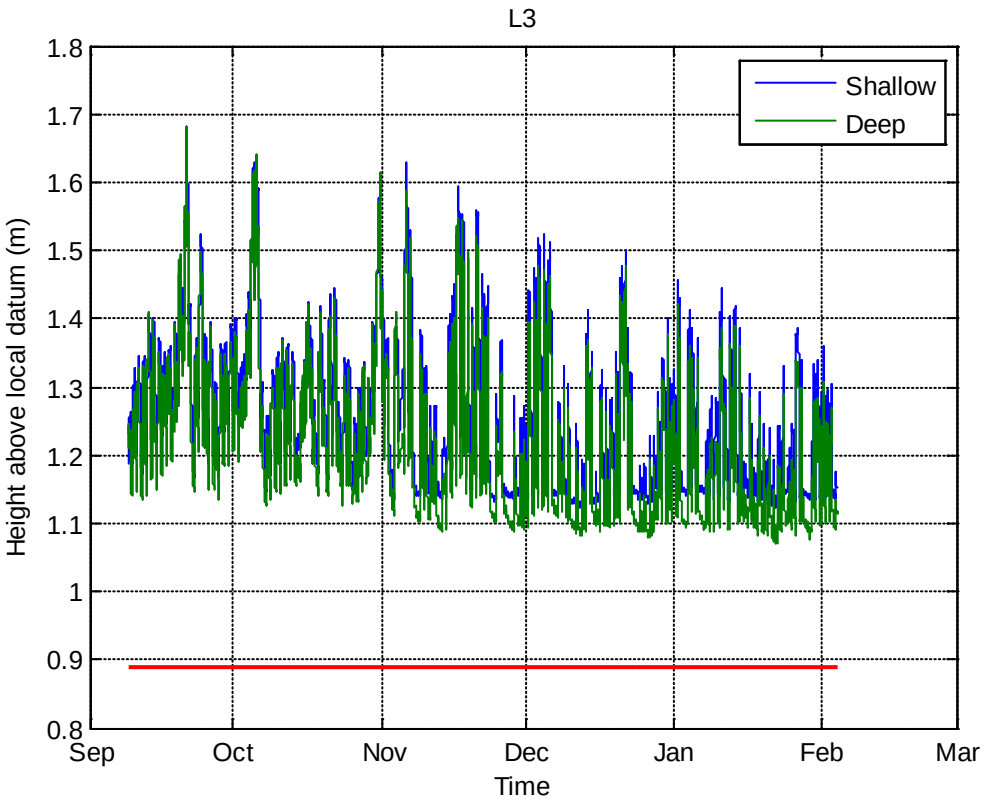
L3
Shallow
Deep
Height above local datum (m)
1.8
1.7
1.6
1.5
1.4
1.3
1.2
1.1
1
0.9
0.8
Sep
Oct
Nov
Dec
Jan
Feb
Mar
Time

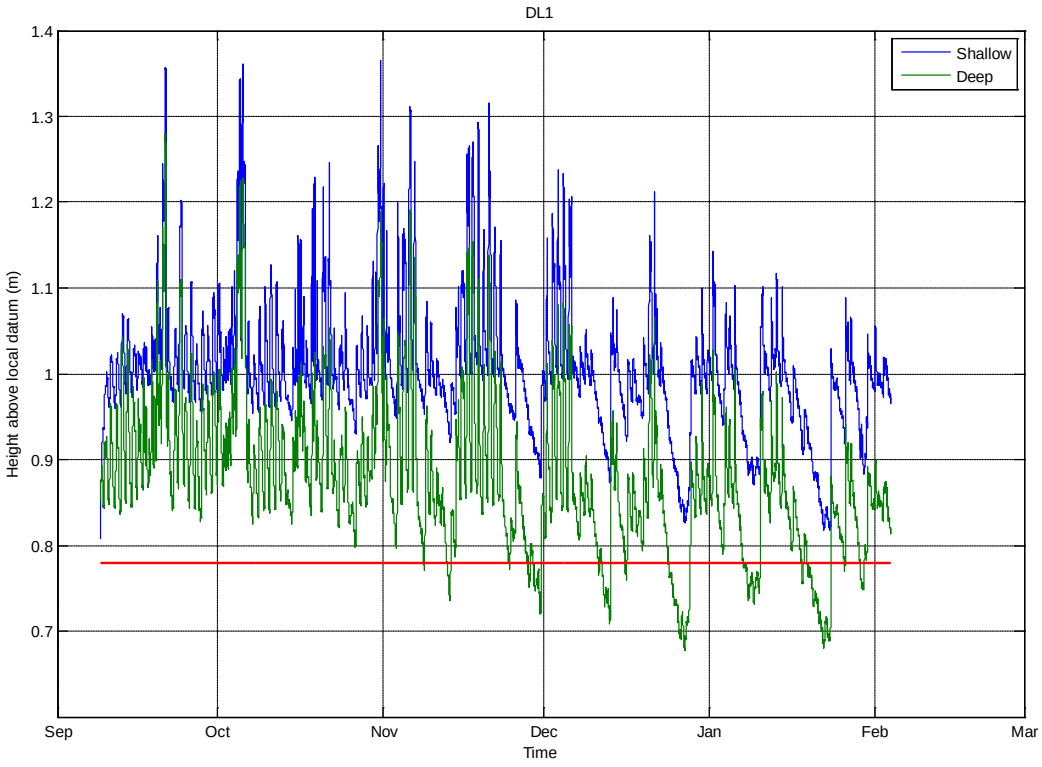
DL1
Shallow
Deep
Height above local datum (m)
1.4
1.3
1.2
1.1
1
0.9
0.8
0.7
Sep
Oct
Nov
Dec
Jan
Feb
Mar
Time

7. References

Alam, M., 1996, Subsidence of the Ganges—Brahmaputra Delta of Bangladesh and Associated Drainage, Sedimentation and Salinity Problems, in Milliman, J.D. and Haq, B.U. eds., Sea-Level Rise and Coastal Subsidence, Coastal Systems and Continental Margins 2, Springer Netherlands, p. 169–192.

Anschutz, P., Smith, T., Mouret, A., Deborde, J., Bujan, S., Poirier, D., and Lecroart, P., 2009, Tidal sands as biogeochemical reactors: Estuarine Coastal and Shelf Science, v. 84, p. 84–90, doi: 10.1016/j.ecss.2009.06.015.

Bardini, L., Boano, F., Cardenas, M.B., Revelli, R., and Ridolfi, L., 2012, Nutrient cycling in bedform induced hyporheic zones: Geochimica et Cosmochimica Acta, v. 84, p. 47–61, doi: 10.1016/j.gca.2012.01.025.

Branhoff, B., 2012, Nitrogen biogeochemistry in a restored Mississippi River delta: A modeling approach: Louisiana State University Department of Oceanography and Coastal Sciences.

Cardenas, M.B., 2010, Lessons from and assessment of Boussinesq aquifer modeling of a large fluvial island in a dam-regulated river: Advances in Water Resources, v. 33, p. 1359–1366, doi: 10.1016/j.advwatres.2010.03.015.

Cardenas, M.B., and Jiang, H., 2011, Wave-driven porewater and solute circulation through rippled elastic sediment under highly transient forcing: Limnology & Oceanography: Fluids & Environments, v. 1, p. 23–37, doi: 10.1215/21573698-1151658.

Day, J.W., Britsch, L.D., Hawes, S.R., Shaffer, G.P., Reed, D.J., and Cahoon, D., 2000, Pattern and process of land loss in the Mississippi Delta: A Spatial and temporal analysis of wetland habitat change: Estuaries, v. 23, p. 425–438, doi: 10.2307/1353136.

Geleynse, N., Hiatt, M., Sangireddy, H., and Passalacqua, P., 2014, Identifying environmental controls on the shoreline of a natural river delta:.

Goolsby, D.A., Battaglin, W.A., Aulenbach, B.T., and Hooper, R.P., 2000, Nitrogen flux and sources in the Mississippi River Basin: Science of The Total Environment, v. 248, p. 75–86, doi: 10.1016/S0048-9697(99)00532-X.

Habib, E., and Meselhe, E., 2006, Stage–Discharge Relations for Low-Gradient Tidal Streams Using Data-Driven Models: Journal of Hydraulic Engineering, v. 132, p. 482–492, doi: 10.1061/(ASCE)0733-9429(2006)132:5(482).

Harvey, J.W., Germann, P.F., and Odum, W.E., 1987, Geomorphological control of subsurface hydrology in the creekbank zone of tidal marshes: Estuarine, Coastal and Shelf Science, v. 25, p. 677–691, doi: 10.1016/0272-7714(87)90015-1.

Henry, K.M., 2012, Linking nitrogen biogeochemistry to different stages of wetland soil development in the Mississippi River delta, Louisiana. Chapter 5. A conceptual model of biogeochemical cycling during delta development in the Anthropocene [Ph.D. Dissertation]: Louisiana State University, 166 p.

Hiatt, M.R., Wagner, R. Wayne, Geleynse, Nathanial, Minton, Brandon, and Passalacqua, Paola, 2014, A network-based analysis of river delta surface hydrology : an example from Wax Lake Delta:.

Horn, D.P., 2002, Beach groundwater dynamics: Geomorphology, v. 48, p. 121–146, doi: 10.1016/S0169-555X(02)00178-2.

Hughes, C.E., Binning, P., and Willgoose, G.R., 1998, Characterisation of the hydrology of an estuarine wetland: Journal of Hydrology, v. 211, p. 34–49, doi: 10.1016/S0022-1694(98)00194-2.

Kim, W., Mohrig, D., Twilley, R., Paola, C., and Parker, G., 2009, Is It Feasible to Build New Land in the Mississippi River Delta?: Eos, Transactions American Geophysical Union, v. 90, p. 373–374, doi: 10.1029/2009EO420001.

Li, L., and Barry, D.A., 2000, Wave-induced beach groundwater flow: Advances in Water Resources, v. 23, p. 325–337, doi: 10.1016/S0309-1708(99)00032-9.

Li, S., Wang, G., Deng, W., Hu, Y., and Hu, W.-W., 2009, Influence of hydrology process on wetland landscape pattern: A case study in the Yellow River Delta: Ecological Engineering, v. 35, p. 1719–1726, doi: 10.1016/j.ecoleng.2009.07.009.

Louisiana's 2012 Coastal Master Plan.

McCarthy, T.S., 2006, Groundwater in the wetlands of the Okavango Delta, Botswana, and its contribution to the structure and function of the ecosystem: Journal of Hydrology, v. 320, p. 264–282, doi: 10.1016/j.jhydrol.2005.07.045.

Moffett, K.B., Gorelick, S.M., McLaren, R.G., and Sudicky, E.A., 2012, Salt marsh ecohydrological zonation due to heterogeneous vegetation–groundwater–surface water interactions: Water Resources Research, v. 48, p. W02516, doi: 10.1029/2011WR010874.

Musslewhite, C.L., McInerney, M.J., Dong, H., Onstott, T.C., Green-Blum, M., Swift, D., Macnaughton, S., White, D.C., Murray, C., and Chien, Y.-J., 2003, The Factors Controlling Microbial Distribution and Activity in the Shallow Subsurface: Geomicrobiology Journal, v. 20, p. 245–261, doi: 10.1080/01490450303877.

NCALM, 2009, Lidar Dataset, Wax Lake Delta: National Center for Airborne Laser Mapping.

Neill, C.F., and Allison, M.A., 2005, Subaqueous deltaic formation on the Atchafalaya Shelf, Louisiana: Marine Geology, v. 214, p. 411–430, doi: 10.1016/j.margeo.2004.11.002.

NGS, 2014, OPUS: the Online Positioning User Service, process your GNSS data in the National Spatial Reference System:.

Nichols, G., 2013, Sedimentology and Stratigraphy: John Wiley & Sons, 808 p.

NOAA, 2014, Tide Predictions - Point Chevreuil 8764634 Tidal Data Daily View - NOAA Tides & Currents:.

Oppenheim, A.V., and Schafer, R.W., 2009, Discrete-Time Signal Processing: Upper Saddle River, Prentice Hall, 1120 p.

Parker, G., and Sequeiros, O., 2006, Large scale river morphodynamics: Application to the Mississippi Delta, in Alves, E., Cardoso, A., Leal, J., and Ferreira, R. eds., River Flow 2006, Taylor & Francis.

Postma, D., Boesen, C., Kristiansen, H., and Larsen, F., 1991, Nitrate Reduction in an Unconfined Sandy Aquifer: Water Chemistry, Reduction Processes, and Geochemical Modeling: Water Resources Research, v. 27, p. 2027–2045, doi: 10.1029/91WR00989.

Rabalais, N.N., Turner, R.E., JustiĆ, D., Dortch, Q., Wiseman, W.J., and Gupta, B.K.S., 1996, Nutrient changes in the Mississippi River and system responses on the adjacent continental shelf: Estuaries, v. 19, p. 386–407, doi: 10.2307/1352458.

Reed, D.J., 2002, Sea-level rise and coastal marsh sustainability: geological and ecological factors in the Mississippi delta plain: Geomorphology, v. 48, p. 233–243, doi: 10.1016/S0169-555X(02)00183-6.

Reide Corbett, D., Dillon, K., and Burnett, W., 2000, Tracing Groundwater Flow on a Barrier Island in the North-east Gulf of Mexico: Estuarine, Coastal and Shelf Science, v. 51, p. 227–242, doi: 10.1006/ecss.2000.0606.

Rivera-Monroy, V.H., Lenaker, P., Twilley, R.R., Delaune, R.D., Lindau, C.W., Nuttle, W., Habib, E., Fulweiler, R.W., and Castañeda-Moya, E., 2010, Denitrification in coastal Louisiana: A spatial assessment and research needs: Journal of Sea Research, v. 63, p. 157–172, doi: 10.1016/j.seares.2009.12.004.

Roberts, H.H., Walker, N., Cunningham, R., Kemp, G.P., and Majersky, S., 1997, Evolution of sedimentary architecture and surface morphology: Atchafalaya and Wax Lake Deltas, Louisiana (1973-1994): Gulf Coast Association of Geological Societies Transactions, v. 47, p. 8.

Röper, T., Kröger, K.F., Meyer, H., Sültenfuss, J., Greskowiak, J., and Massmann, G., 2012, Groundwater ages, recharge conditions and hydrochemical evolution of a barrier island freshwater lens (Spiekeroog, Northern Germany): Journal of Hydrology, v. 454–455, p. 173–186, doi: 10.1016/j.jhydrol.2012.06.011.

Shaw, J.B., Mohrig, D., and Whitman, S.K., 2013, The morphology and evolution of channels on the Wax Lake Delta, Louisiana, USA: Journal of Geophysical Research: Earth Surface, v. 118, p. 1562–1584, doi: 10.1002/jgrf.20123.

Siebert, S., Burke, J., Faures, J.M., Frenken, K., Hoogeveen, J., Döll, P., and Portmann, F.T., 2010, Groundwater use for irrigation – a global inventory: Hydrol. Earth Syst. Sci., v. 14, p. 1863–1880, doi: 10.5194/hess-14-1863-2010.

Slingerland, R., and Smith, N.D., 2004, River Avulsions and Their Deposits: Annual Review of Earth and Planetary Sciences, v. 32, p. 257–285, doi: 10.1146/annurev.earth.32.101802.120201.

Smith, B., 2014, The effect of vegetation on delta morphology [M.S. Thesis]: The University of Texas at Austin.

Snedden, G., 2006, River, Tidal, and Wind Interactions on a Deltaic Estuarine System: Louisiana State University Department of Oceanography and Coastal Sciences.

Spalding, R.F., and Parrott, J.D., 1994, Shallow groundwater denitrification: Science of The Total Environment, v. 141, p. 17–25, doi: 10.1016/0048-9697(94)90014-0.

Stanley, D.J., 1990, Recent subsidence and northeast tilting of the Nile delta, Egypt: Marine Geology, v. 94, p. 147–154, doi: 10.1016/0025-3227(90)90108-V.

Syvitski, J.P.M., and Saito, Y., 2007, Morphodynamics of deltas under the influence of humans: Global and Planetary Change, v. 57, p. 261–282, doi: 10.1016/j.gloplacha.2006.12.001.

Ursino, N., Silvestri, S., and Marani, M., 2004, Subsurface flow and vegetation patterns in tidal environments: Water Resources Research, v. 40, p. W05115, doi: 10.1029/2003WR002702.

USGS, 2014, USGS Current Conditions for USGS 07381490 Atchafalaya River at Simmesport, LA:.

Venterink, H.O., Hummelink, E., and Hoorn, M.W.V.D., 2003, Denitrification potential of a river floodplain during flooding with nitrate-rich water: grasslands versus reedbeds: Biogeochemistry, v. 65, p. 233–244, doi: 10.1023/A:1026098007360.

Viparelli, E., Shaw, J., Bevington, A., Meselhe, E., Holm, G., Mohrig, D., Twilley, R., and Parker, G., 2011, Inundation Model As an Aid for Predicting Ecological Succession on Newly-Created Deltaic Land Associated with Mississippi River Diversions: Application to the Wax Lake Delta, in World Environmental and Water Resources Congress 2011, American Society of Civil Engineers, p. 2340–2349.

Wada, Y., van Beek, L.P.H., Sperna Weiland, F.C., Chao, B.F., Wu, Y.-H., and Bierkens, M.F.P., 2012, Past and future contribution of global groundwater depletion to sea-level rise: Geophysical Research Letters, v. 39, p. L09402, doi: 10.1029/2012GL051230.

Wellner, R., Beaubouef, R., Van Wagoner, J., Roberts, H., and Sun, T., 2005, Jet-plume depositional bodies—the primary building blocks of Wax Lake Delta: Gulf Coast Association of Geological Societies Transactions, v. 55, p. 867–909.

William P. Anderson, 2002, Aquifer Salinization from Storm Overwash: Journal of Coastal Research, v. 18, p. 413–420, doi: 10.2307/4299090.

Wilson, A.M., Moore, W.S., Joye, S.B., Anderson, J.L., and Schutte, C.A., 2011, Storm-driven groundwater flow in a salt marsh: Water Resources Research, v. 47, p. W02535, doi: 10.1029/2010WR009496.

Zhang, H., Moffett, K.B., Windham-Myers, L., and Gorelick, S., 2013, Hydrological controls on methylmercury flux from an intertidal salt marsh: AGU Fall Meeting Abstracts, v. -1, p. 03.